A Multidisciplinary Approach to Reservoir Characterization of the Coastal Entrada Erg-Margin Gas Play, Utah

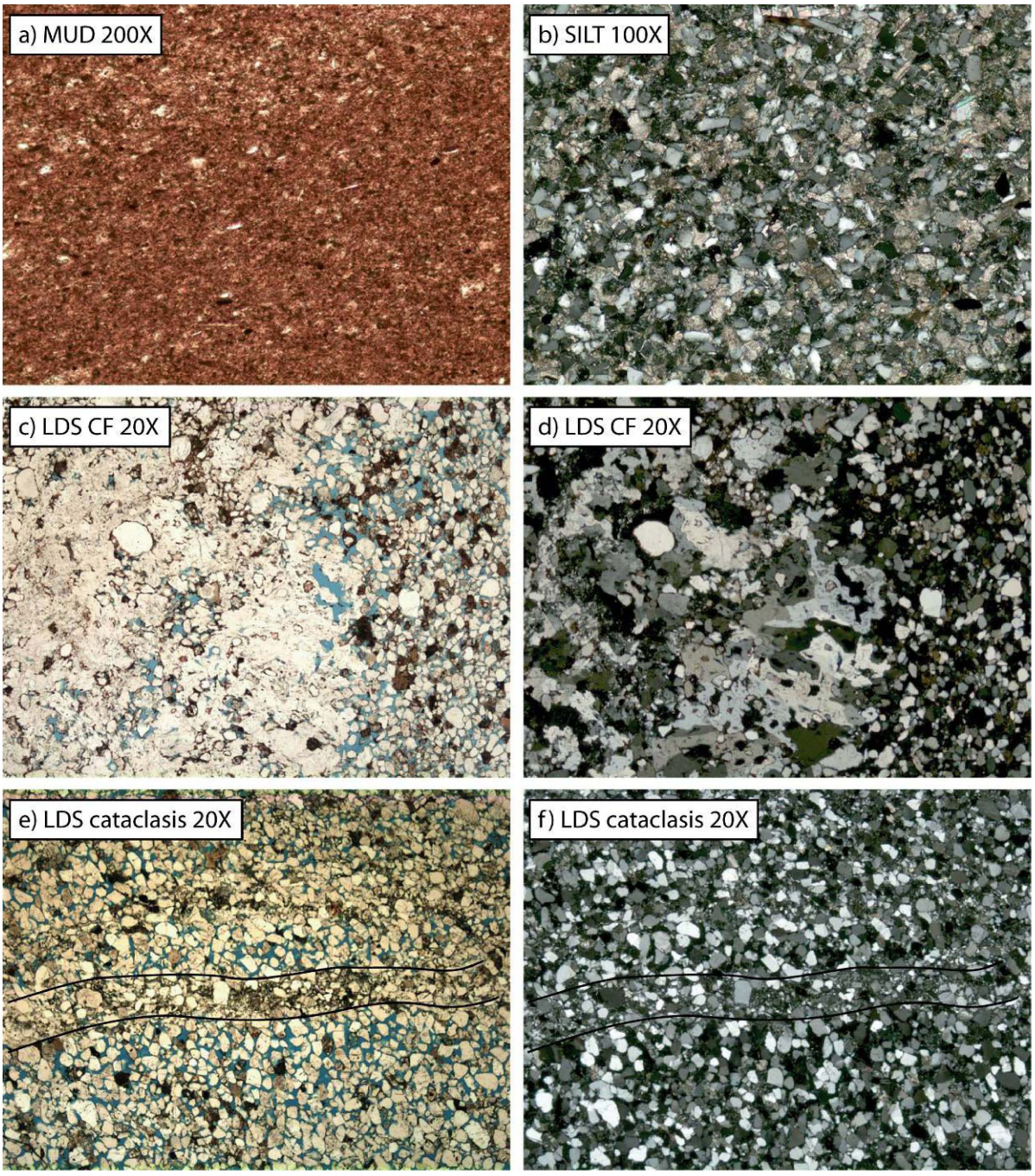

OPEN-FILE REPORT 459 September 2005
Utah Geological Survey
a division of
Utah Department of Natural Resources

A Multidisciplinary Approach to Reservoir Characterization of the Coastal Entrada Erg-Margin Gas Play, Utah

THOMAS H. MORRIS (PI)
JOHN H. MCBRIDE (Co-PI)
WILL D. MONN (MS Candidate)

Department of Geology, Brigham Young University, Provo, UT, 84602, USA

Utah Geological Survey (UGS)
"Characterization of Utah's Natural Gas Reservoirs and Potential New Reserves"
Contract # 051844

June 29, 2005

Disclaimers

This open-file report was prepared on a contract basis with the author(s) and the Utah Department of Natural Resources, Utah Geological Survey, contract number 051844. The report has not been reviewed for technical quality by professional scientists and is being made available to the public as submitted to the Utah Geological Survey.

This open-file report makes information available to the public, which may not conform to Utah Department of Natural Resources, Utah Geological Survey policy, editorial, or technical standards. Therefore, it may be premature for an individual or group to take action based on its content.

Although this product represents the work of professional scientists, the Utah Department of Natural Resources, Utah Geological Survey, makes no warranty, expressed or implied, regarding its suitability for a particular use. The Utah Department of Natural Resources, Utah Geological Survey, shall not be liable under any circumstances for any direct, indirect, special, incidental, or consequential damages with respect to claims by users of this product.

TABLE OF CONTENTS

Headings

Figures

Tables

Appendicies

ABSTRACT

The Jurassic Entrada erg-margin contains isolated reservoir quality sandstone bodies. These high quality reservoirs are dominated by eolian-influenced facies. They are sealed vertically and laterally by muddy facies of associated tidal flat deposits. Thus, these sandstones can become excellent stratigraphic traps in the subsurface. The Entrada erg-margin trend runs from the northeast portion to the south-central portion of Utah.

A variety of approaches were used to characterize the Entrada erg-margin gas play in the State of Utah. In the outcrop case study these approaches include: annotated photomosaic panoramas of outcrops, measured sections, scintillometer measurements of field sections, facies analysis, grain size analyses, paleocurrent analysis, 2D high resolution shallow seismic surveys, porosity and permeability analysis, sedimentary petrography, and sedimentary petrology. Logs from the North Hill Creek/Flat Rock (NHC/FR) field, located in the southern Uinta Basin, Utah were analyzed and correlated to the outcrop study.

The outcrop study area appears to be an excellent analog to the NHC/FR field with the possible exception that the outcrop study area may be located in the central portion of the erg-margin trend while the NHC/FR field is located nearer the erg proper. Seven facies are identifiable in outcrop. The small dune set (SDS), large dune set (LDS), and upper ripple laminated (URL) facies are the volumetrically most important facies of the reservoir quality sandstone bodies and display the highest quality porosity and permeability. They are feldspathic arenites. Many of the sandstone bodies within the outcrop belt are genetically related and probably in communication with each other. This results from dune complex migration through time. Dune complex migration is interpreted from measured sections and 2D seismic imaging. Hence, dune complexes shifted locations both geographically and stratigraphically through time.

Thicker sandstone bodies seen in outcrop are more likely to be connected to migrating dune complexes. The size of one of these complexes in the case study area is estimated to be larger than 13 million cubic meters in volume. Small sandstone bodies are much more likely to be isolated from large dune complexes and may be as small as 31 thousand cubic meters. An amplitude time slice through the Entrada Sandstone from the NHC/FR field 3D seismic survey suggests that these dune complexes are composed of star dunes, barcanoid dunes and/or linear/seif dunes. Fracture sets and small-scale faults may act as baffles and barriers as they cross-cut facies in outcrop exposures. Numerous "suggested practices" are herein proposed in an effort to aid exploration and development strategies of the Entrada erg-margin gas play.

INTRODUCTION

Recent discovery of high btu gas-charged Jurassic reservoirs in the North Hill Creek/Flat Rock (NHC/FR) field located in the southern Uinta basin, Utah have ignited interest in below-Tertiary reservoirs within the basin and in other areas of Utah. Eleven wells in the NHC/FR field have penetrated the productive Jurassic Entrada sandstone interpreted to be associated with the coastal erg-margin. This interpretation came about from close examination of amplitude time slices from a 3D seismic data set, close analysis of the associated well logs, and previous field studies (Marc Eckels, Wind River Resources, personal communication, 2005). Ancient erg-margins are of particular interest because of their potential to contain large, high quality reservoirs. Further, erg-margin sandstones have been recognized as potential stratigraphic and combination hydrocarbon traps especially when they are laterally associated with muddy, marine-influenced facies (Fryberger, 1986; Chan, 1989; Mariño and Morris, 1996). High potential for further development of this play exists along a north-south trend extending from the

Uinta basin through southern Utah (Kocurek, 1981; Eschner and Kocurek, 1986; Blakey, 1988; Peterson, 1988).

Entrada erg-margin sandstones exposed in outcrop along the east flank of the Waterpocket Fold near Capitol Reef National Park appear to be isolated sandstone bodies enveloped within a tidal flat "earthy" facies (Fig. 1). The earthy facies around the sandstone bodies are dominated by dirty sandstones, siltstones, and mudstones. Since these outcrops appear to be analogs for reservoirs in the NHC/FR field, we chose to use them as a case study area. In order to better constrain the location of this coastal erg-margin, an extensive literature search was completed for articles discussing the location of the coastal erg-margin trend of the Entrada Sandstone in Utah. Using our own knowledge of the Entrada system and articles from Kocurek (1981), Eschner and Kocurek (1986), Blakey (1988), and Peterson (1988), along with the paleogeographic maps they provided, a fairway map was created that establishes the location of the Entrada erg-margin in Utah (Fig. 2).

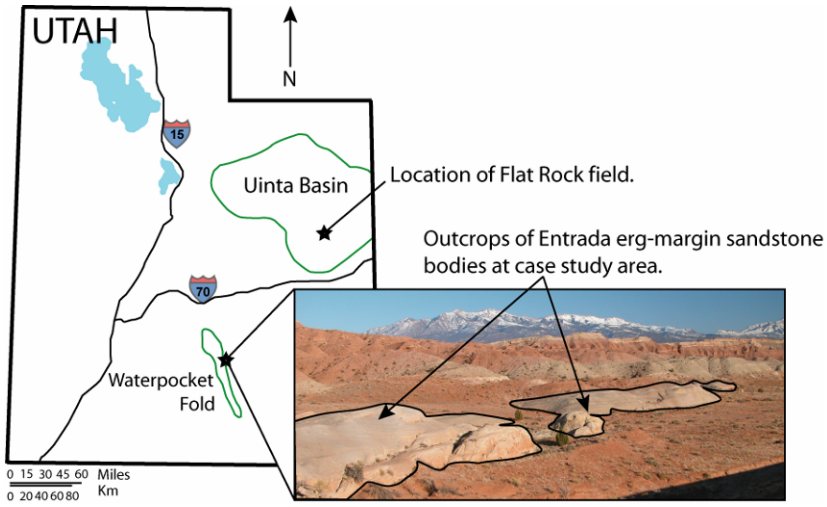

Figure 1. Index map displaying the locations of the NHC/FR field and the case study outcrop.

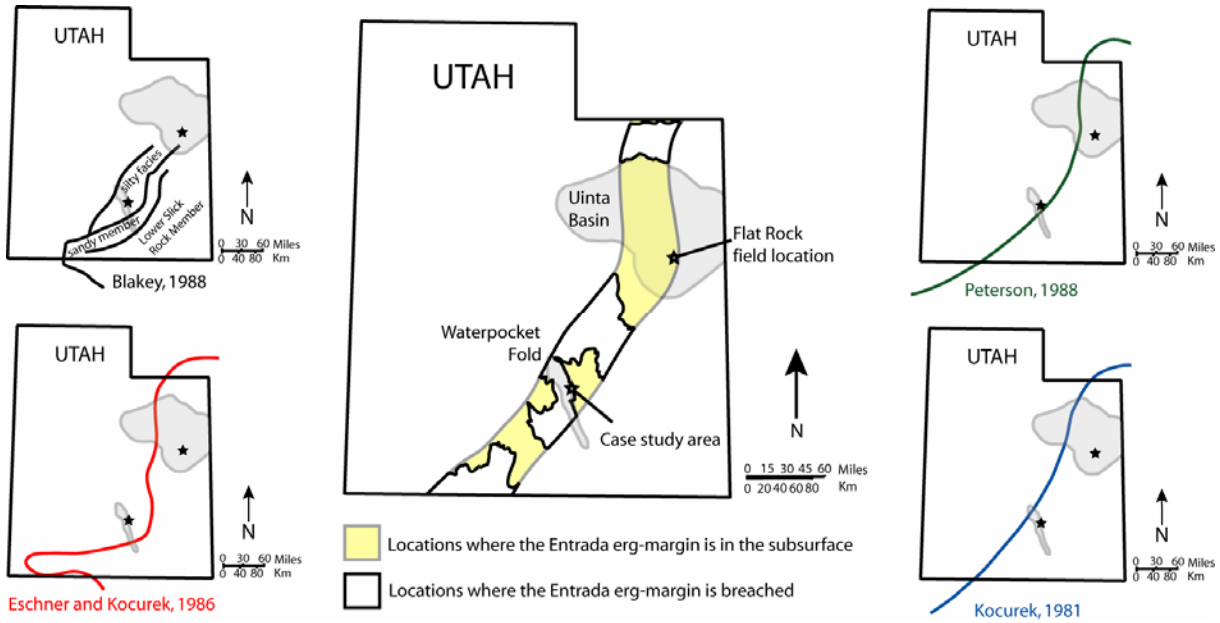

Figure 2. The Entrada erg-margin location was estimated based on a literature search and our own data. The yellow and white band represents the Entrada erg-margin which has high stratigraphic trap potential. Continuous erg facies of the Entrada lie to the east of the yellow and white band while muddy tidal flat facies lie to the west.

METHODS

A multidisciplinary research approach was used to further knowledge of the Entrada erg-margin play and to characterize reservoir quality rocks associated therein. We began by looking at the sandstone body geometries through outcrop panoramics and by measuring stratigraphic sections in 12 locations over the extent of the outcrop. For more information on the sandstone body dimensions, three high resolution seismic reflection surveys were completed in locations where the case study outcrop extended into the subsurface. For reservoir quality information of the outcrop sandstones, facies were closely studied and thoroughly sampled for laboratory analysis. Finally, well log data from the NHC/FR field was examined and compared to data from the case study outcrop.

First, we separated the 2.5 km outcrop into two fields, labeled as the North Field and the South Field (Fig 3). The North Field consists of six relatively small sandstone bodies that lie

approximately 0.5 km to the north of the South Field, which consists of six relatively large sandstone bodies. Sandstone body identifications (e.g. NF-1) were based on the field they are in and their relative position in that field (Fig. 3).

Sandstone Body Geometries

Panoramas. Panoramas were shot from both the North and South Fields and annotated in order to better understand the lateral association of the sandstone bodies as well as to better visualize the Curtis Formation-Entrada Sandstone contact (Fig. 4). As can be seen on the panoramas, drainages cutting between sandstone bodies are backfilled with alluvium causing the bodies to appear isolated from each other. Though some of the sandstone bodies may be separated stratigraphically from the others, we believe that many of them are actually connected in the subsurface. Due to thicknesses (up to 21-25 m in the South Field) and close lateral proximity of the sandstone bodies, it is very likely that they do connect in the subsurface. Further, it is apparent that the sandstone bodies become stratigraphically higher to the south (Fig. 4a). SF-1 and SF-2 are a good distance

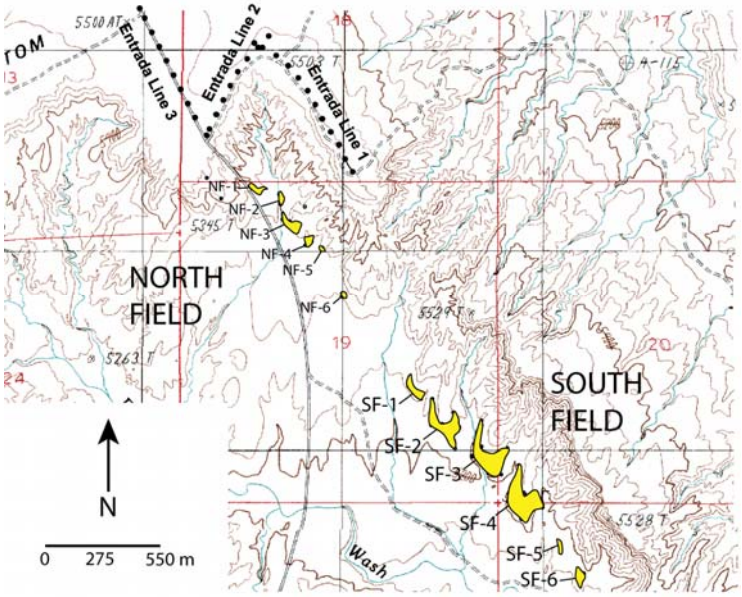

Figure 3. Map showing the case study area and the separation of the two fields along with the sandstone body labels. The locations where the seismic lines were shot are also marked.

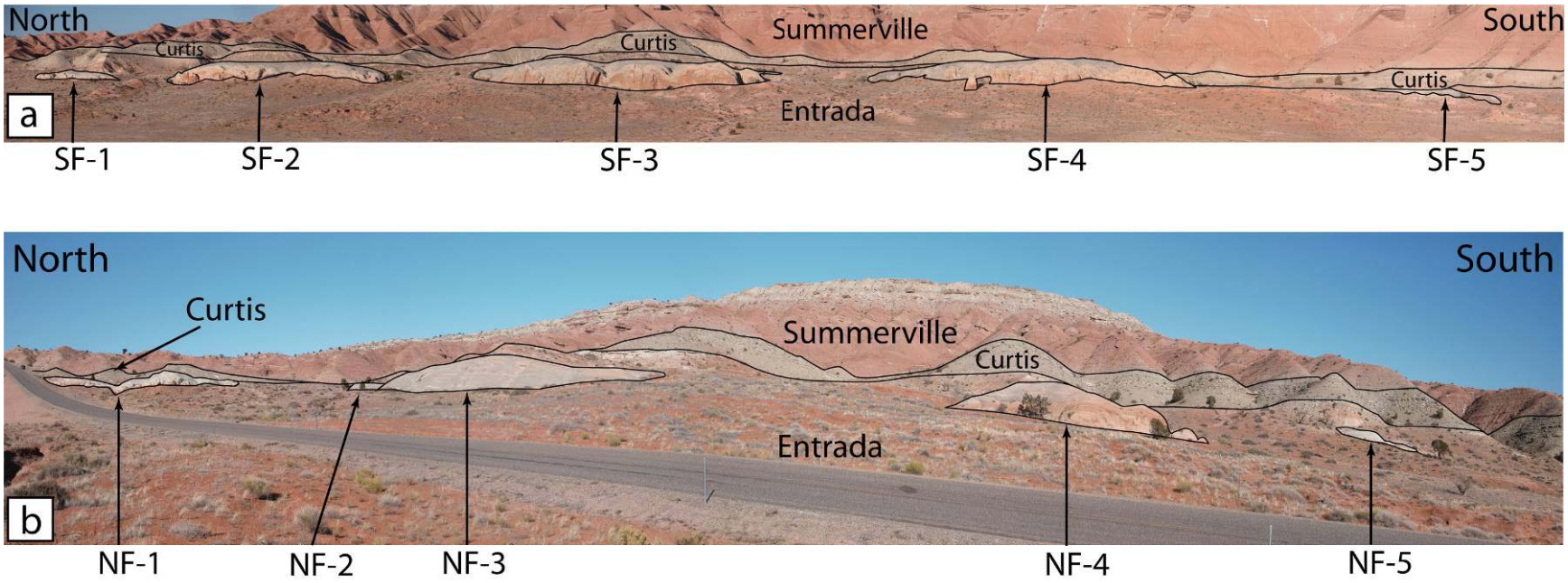

Figure 4. a) Eastward view taken 1 km away from the outcrop. This panoramic of the South Field shows five of the six sandstone bodies and their relationships to the overlying Curtis Formation. SF-1 is significantly below the contact while SF-2 through SF-4 become much closer to the contact until SF-5 is actually touching it. b) Eastward view taken 200 m away from the outcrop. This panoramic of the North Field shows five of the six sandstone bodies and displays the relationship between the Entrada Sandstone and the Curtis. Note that NF-1 is in contact with the Curtis while the other sandstone bodies are not.

below the Curtis-Entrada contact while SF-4 and SF-5 are either just below it or right at the contact.

The North Field also displays a similar relationship; however, it tends to be a little more random and not entirely visible in Figure 4b. NF-3 through NF-5 behave similar to the South Field, yet NF-1, NF-2, and NF-6 appear separated and isolated from any other sandstone bodies. Because all of the outcrop sandstones have eolian characteristics, with the exception of a few intermittent ripple laminated facies, we believe that the sandstone bodies in both fields represent dune complexes that were migrating to the south and up section over time. This interpretation is supported by both paleocurrent analysis of bedforms within the sandstone bodies and the seismic surveys (see below).

Measured Sections. To test and document this migrating-to-the-south relationship, stratigraphic sections were measured from the base of each sandstone body in both fields up through the Curtis Formation. Due to the unconformable contact between the Entrada and Curtis, the sections were measured up to the Curtis-Summerville contact so that there would be a conformable datum from which the sections could be hung and compared (Fig. 5). Stratigraphic relationships can be better visualized when measured stratigraphic sections are hung from the Curtis-Summerville contact and spaced to scale. Figure 5 displays the unconformable relationship of the Curtis-Entrada contact and also illustrates the offset and upward-stepping progression of the sandstone bodies in both fields.

We believe that all of the South Field sandstone bodies, except possibly SF-6, connect in the subsurface based on their stratigraphic relationships. By assuming eolian deposition and interconnected sandstone bodies, one dune complex initiating near SF-1 and migrating to the south over time, depositing sand progressively higher up section, could be responsible for most

of the outcrop in the South Field. This interpretation of continuity between sandstone bodies dramatically increases the size of the South Field reservoir.

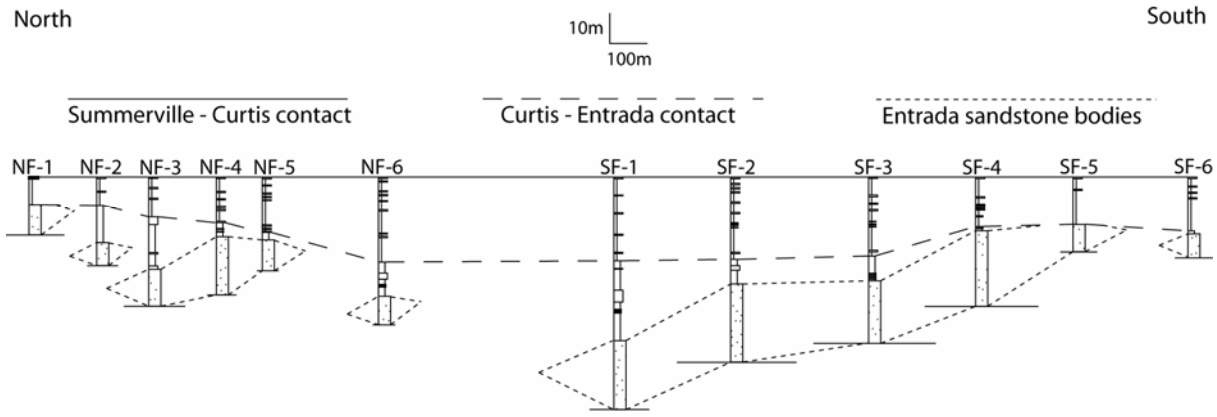

Figure 5. Measured sections hung from the conformable Curtis-Summerville contact. From this figure, the unconformable contact between the Curtis and Entrada can be seen as well as the apparent southward and upward migration of the sandstone bodies. The horizontal lines at the base of each section represent the full surface exposure of each sandstone body. Note that the Curtis sits directly on top of the eolian sandstones in sections NF-1 and SF-5.

The North Field sandstone bodies are notably more isolated than those in the South Field (Fig. 5). In the North Field, several smaller dune complexes are separated from each other. For example, NF-1, NF-2, and NF-6 appear completely disconnected from the other sandstone bodies while NF-3 through NF-5 appear connected. Our seismic interpretation suggests that NF-1 is also connected to another southward migrating dune complex at the southern end of seismic Line 3. Thus, similar southward-migrating dune complexes are interpreted to be present both in the North Field and the South Field.

Paleocurrent Analysis. For further evidence of southward migrating dune complexes, a paleocurrent analysis was completed. Paleocurrent directional data was gathered from the foresets of cross-beds from three-dimensional outcrop exposures. Measurements were taken from different sets through the vertical section as well as along strike of the section from separate sandstone bodies in both fields. The strike and dip of the foreset lamina were measured and

corrected for regional structural dip. The reoriented data was completed using a stereogram (Collinson and Thompson, 1982).

The paleocurrent data were separated for both fields in order to see the wind direction associated with each field. We found that both the North and South Fields had a southeasterly wind direction which would have allowed for the southeasterly dune migration pattern we interpret from measured sections (Figs. 5 & 6).

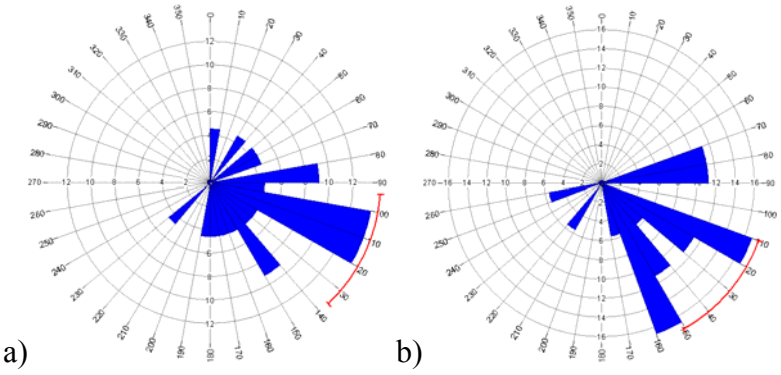

a) b)

Figure 6. a) North Field rose plot created from 22 data points. The standard deviation is 3.27% with a vector mean of 115 degrees. b) South Field rose plot from 18 data points. The standard deviation is 4.38% with a vector mean of 130 degrees. Concentric circles represent percent of observations falling into a particular 10 degree bin.

Seismic Survey. From our measured sections and panoramas we obtained good 2D constraints on the geometry and connectivity of the sandstone bodies in both fields. In an effort to obtain a third dimension to the sandstone body geometries, we used 2D seismic reflection surveys that were shot behind and adjacent to the outcrop where it extends into the subsurface. Three high-resolution compressional wave (P-wave) seismic reflection surveys were shot along and just east of Notom Road where the outcrop dips into the subsurface (Figs. 3, 7, 8, & 9). Line 1 (~803 m) was shot along strike on a dirt road on the top of a ridge behind the outcrop while Line 2 (~562 m) was shot on a dirt road that parallels the dip of the outcrop. Line 3 (~584 m), also a strike line, was shot on Notom Road just north of the outcrop (Fig. 3). The seismic source used for the acquisition of this data was an ATV-mounted 100-lb accelerated elastic weight dropper ("Seispulse"), stacked twice. The seismic source and geophone spacing was 10 ft with 48 recording channels giving a nominal fold of cover of 24. Receivers included one 28-Hz

geophone per group. A full explanation of the method can be found in *Geophysical Prospecting* by Dobrin and Savit (1988).

The reflection surveys were performed by Brigham Young University students and faculty under the supervision of John McBride. The data processing includes: trace editing, refraction and elevation statics (datum = 1700 m above sea level), mute, bandpass frequency and dip filtering, deconvolution, normal move-out correction, common midpoint (CMP) stack, depth conversion, and display as color amplitude sections.

Seismic interpretations. Line 1 was the first seismic line to be interpreted because accurate stratal thickness for the underlying Morrison, Summerville, and Curtis formations could be measured on the slope just below where the line was shot. The Curtis thickness was approximately 5-15 m while the Summerville was approximately 80-90 m thick. Small scale faults within the Summerville section make the measurement of its thickness somewhat tenuous. We estimate that fault offsets could change the overall thickness by +/- 5-10 m. A thin stratal portion of the Morrison, which lies on top of the Summerville, caps the ridge. Its thickness was found to vary from 1 to 5 m over the extent of Line 1. Seismic interpretation of the sandstone bodies was based upon the relationship of reflectors onlapping/truncating onto positive features. We expected the sandstone bodies to be near the base of the seismic resolution.

Using measured thicknesses from outcrop, reflectors for each formation were picked and traced over Line 1. Because Lines 1 and 2 intersect near their northern ends, the formation reflectors could be correlated between profiles. Lines 2 and 3 were also correlated even though the southern end of the lines missed crossing each other by approximately 30 m.

With the appropriate measured thicknesses emplaced it is apparent that seismic resolution deteriorates within the upper Entrada Sandstone (Figs. 7, 8, & 9). This fading out of the reflectors is partly attributed to rapid attenuation of the seismic signal by the sandstone bodies.

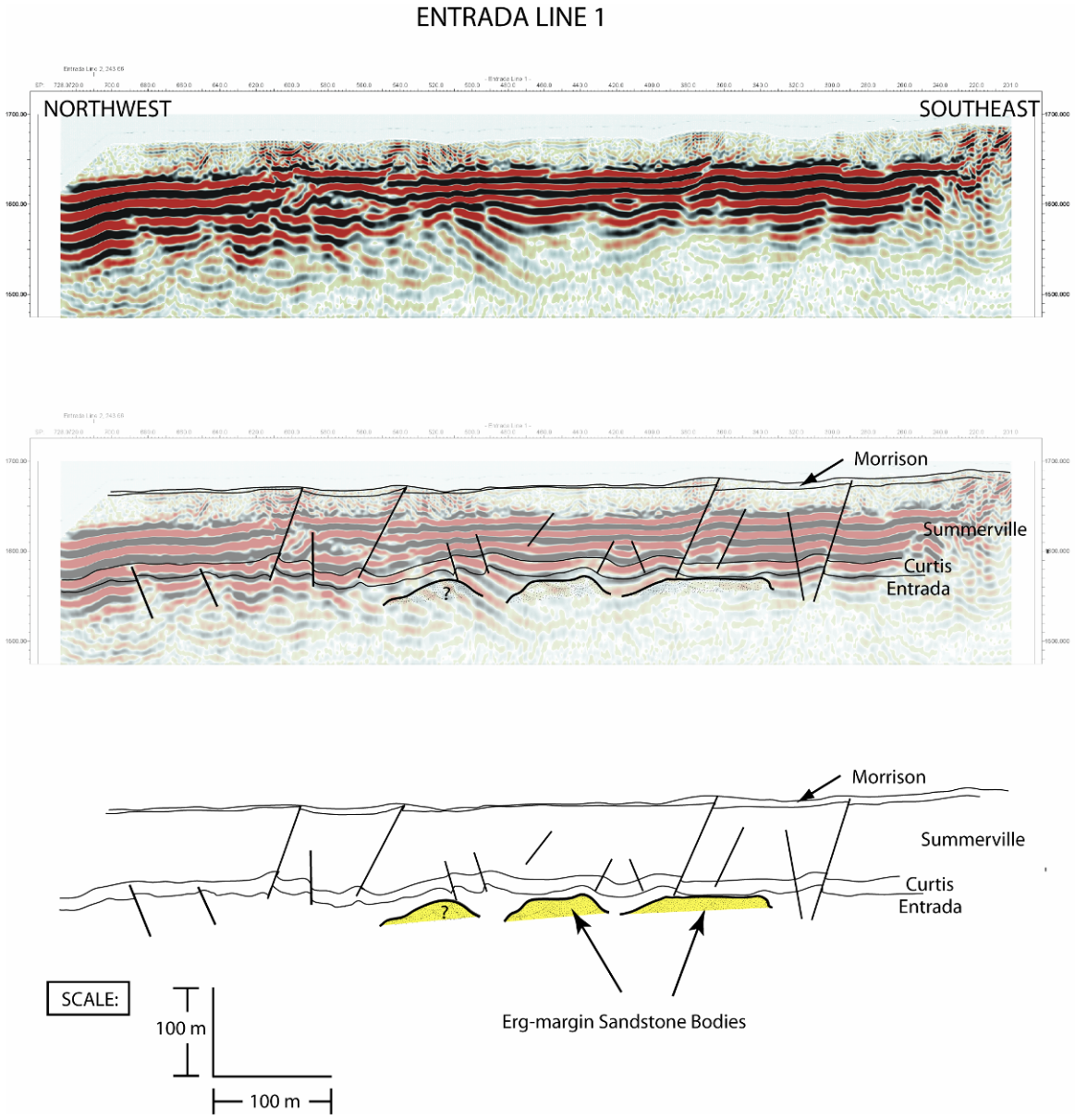

Figure 7. Interpretation of Entrada seismic Line 1.

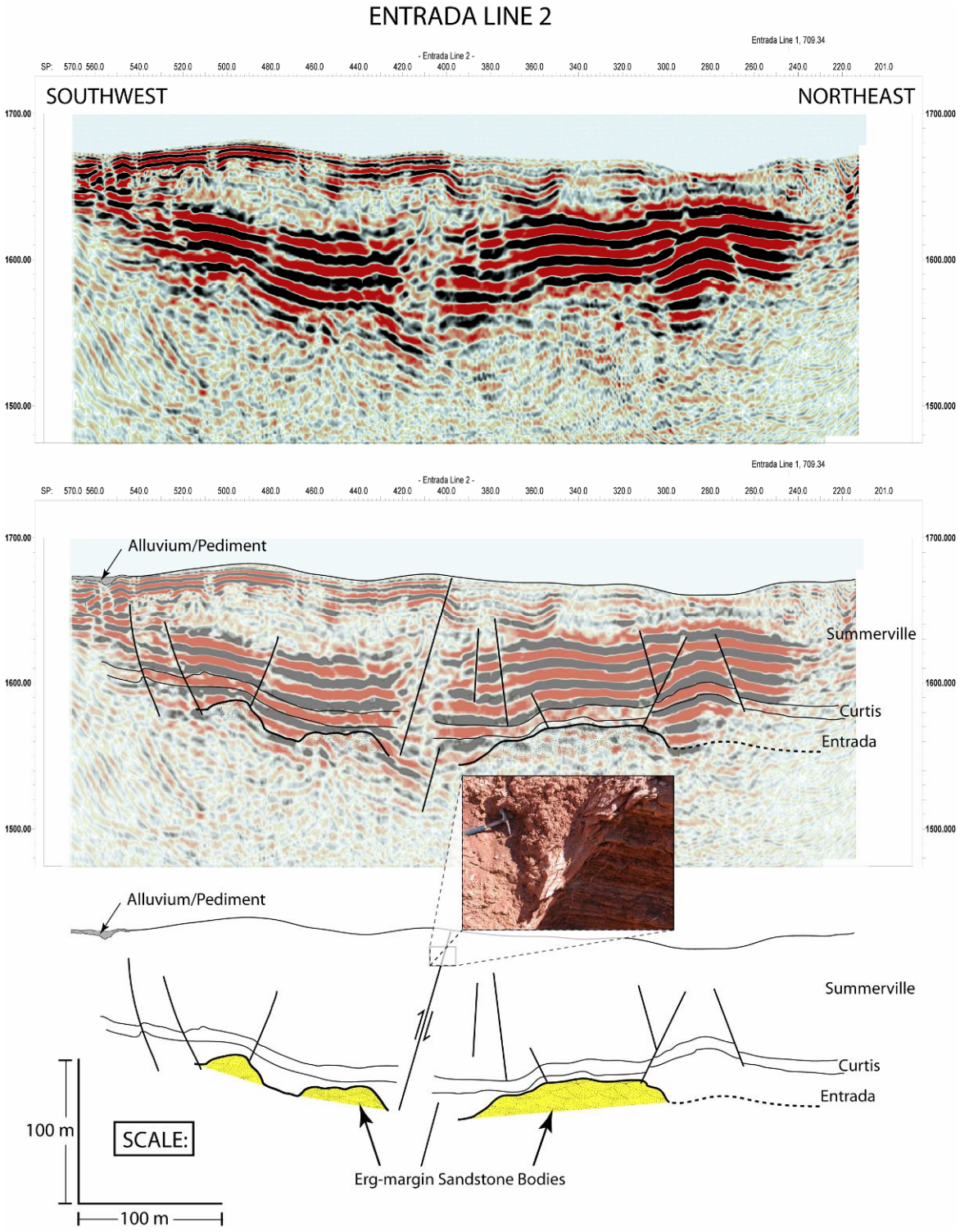

Figure 8. Interpretation of Entrada seismic Line 2. The reverse fault that is located in the middle of the seismic line was found in outcrop (see inset photo).

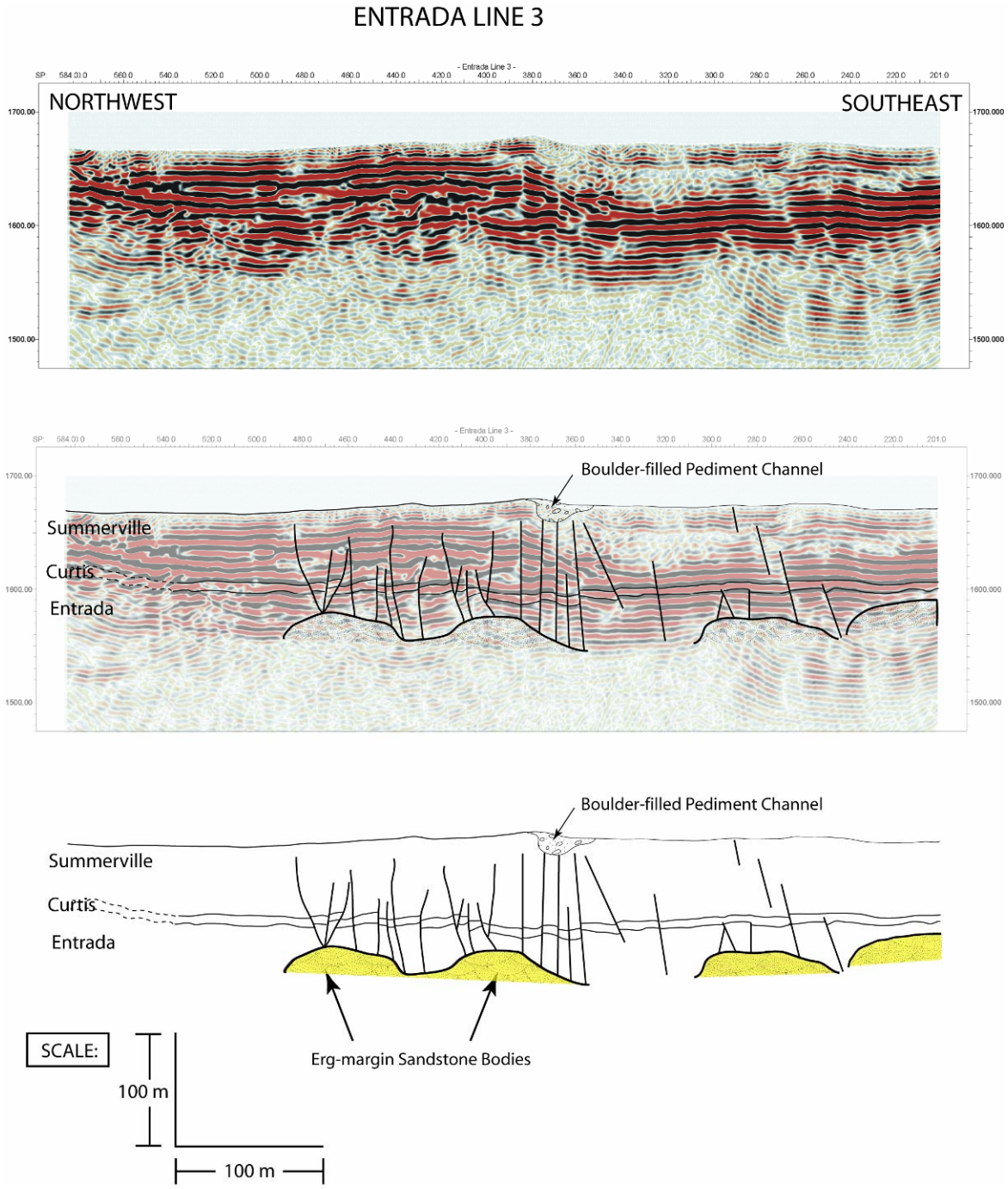

Figure 9. Interpretation of Entrada seismic Line 3. Note the apparent stratigraphic rise of the two sandstone bodies on the southeast end of the survey. The NF-1 outcrop is adjacent to the southeast end of Line 3 and the Curtis Formation sits directly on top of NF-1, suggesting southeastward migration through time.

As seen on the interpreted seismic lines and in outcrop panoramas (Figs. 4 & 7), the sandstone bodies tend to have flat to rounded tops with an overall dome-like shape. This sort of surficial geometry could be due to erosional relief created by Entrada-time tidal flucuations or even the encroaching Curtis seaway and its effect on the water table. This type of relationship is commonly found along the Entrada-Curtis contact (Eschner and Kocurek, 1986; Fryberger, 1986; Eschner and Kocurek, 1988). Areas where there are clear reflectors laterally adjacent to the more fuzzy sandstone bodies are interpreted to be onlapping and alternating tidal deposits of reworked eolian sands with more silt- and mud-rich sediments.

The three seismic surveys indicate that the dune complex continues at least 0.5 km to the north and east. However, in only one case are we able to unequivocally connect seismically imaged sandstone bodies to those of the outcrop (two sandstone bodies at the southern end of Line 3 with NF-1; Figure 9). We expect sandstone bodies imaged in Line 1 to be related to sandstone bodies in the North Field. Line 1 is oriented perpendicular to the migration direction of the dune complexes and the imaged bodies could represent the edges or centers of elongate dune complexes. They would most likely represent the center of the dune complexes due to their greater thicknesses. There is the possibility that some of the bodies found in Lines 2 and 3 connect. Both of these lines image bodies with similar morphology and size that are relatively close to each other.

Rock Body Volumes. High and low estimates of rock body volumes are presented in Table 1. The high case scenario assumes that sandtone bodies SF-1 through SF- 5 are in communication and represent a dune complex. The length of the exposure is approximated at 1.3 km, the thickness is an average of the maximum measured thickness of the five bodies, and the lateral extent of the dune complex is estimated at 0.5 km based on the interpretation of sandstone bodies

being present in seismic Line 1 (which is set back 0.5 km from the NF exposures). Given the possibility that the sandstone bodies extend further than 0.5 km into the subsurface, or are thicker in places, the high case scenario could be significantly underestimated.

Table 1. Summary of high-low scenarios for a dune complex and an isolated dune in the case study area.

ROCK VOLUMES	
High Case Scenario (SF-1-5)	*Low Case Scenario (NF-6)*
Length (Outcrop Exposure) = 1300m Thickness (Average of 5 bodies) = 20.5m Width (Subsurface Extent) = 500m	Length (Outcrop Exposure) = 28m Thickness (One half of max.) = 4.5m Width (Subsurface Extent) = 250m
Rock Body Volume .....13, 325,000 m^3	***Rock Body Volume ..... 31,500 m^3***

The low case scenario assumes that NF-6 is completely isolated from other sandstone bodies. The length of the exposure is only 28 m, the thickness is assumed to be one half of its maximum thickness (9 m), and the lateral extent into the subsurface is 250 m.

These two scenarios illustrate the high variability of subsurface reservoir size that may be expected in the central portion of the Entrada erg-margin. Based on our outcrop work and 2D seismic interpretation, we suggest that there is a positive relationship between the thickness of a given sandstone body and the potential that it is associated with a large dune complex. The smaller the thickness of a sandstone body, the more likely it is isolated from a large dune complex. Figure 10a, a modern analog to our study area, illustrates this relationship. Further, a time slice through the Entrada Sandstone in the NHC/FR field 3D seismic survey suggests that these volume scenarios are plausible (Fig. 10b).

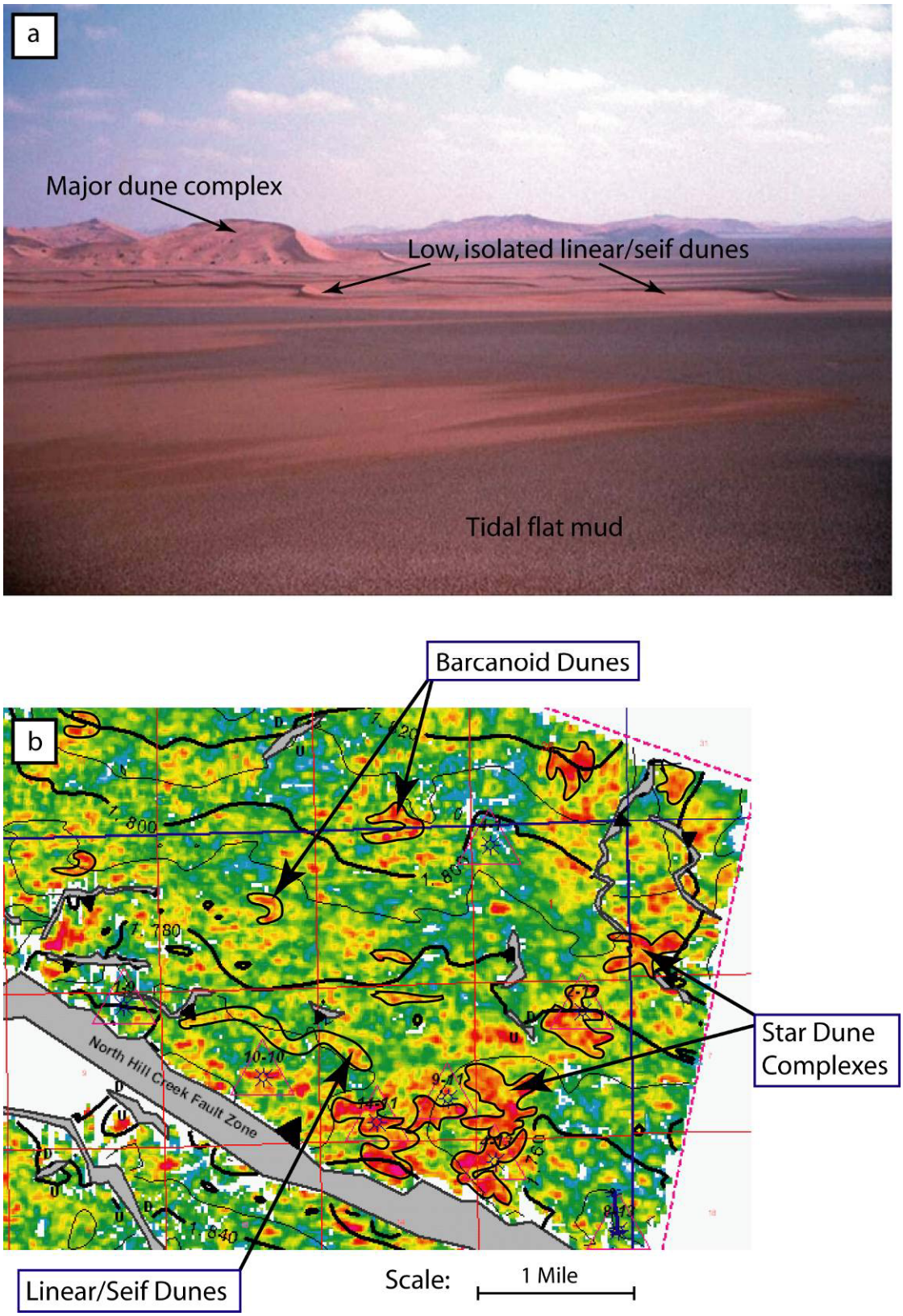

Figure 10. a) Working depositional model with eolian dunes encroaching on a tidal flat, Namibia Desert (photo courtesy of Marc Eckels, Wind River Resources as originally taken from E. Tad Nichols, USGS Prof. Paper 1052). b) "Entrada" Time Slice – North Hill Creek/Flat Rock Field (modified from and courtesy of Marc Eckels, Wind River Resources).

Sampling Reservoir Quality

Facies were identified and sampled over the extent of the outcrop in order to gain information about the reservoir quality of the rocks being studied. Starting from the base of the outcrop, these facies include: MUD = Mudstone facies, BCB = Basal Convolute Bedding, BRL = Basal Ripple Laminated, SDS = Small Dune Sets, LDS = Large Dune Sets, URL = Upper Ripple Laminated, UNS = Upper Non-Resistant Sandstones, RLC = Ripple Laminated Channel, and SILT = Siltstone facies. Not all of these facies are present in both the North and South Fields. The North Field tends to have thinner sandstone bodies, 7.5-12 m thick, and does not display all of the facies found in the South Field. The South Field sandstone bodies are around 21-25 m thick and contain the BCB and BRL facies not found in the North Field.

In order to accurately describe and understand these facies, bulk samples were collected from each facies for grain size and thin section analysis. Where possible, core plugs were collected with a 1 inch diameter core drill for porosity and permeability tests.

Grain Size. Due to the friability of the rocks, the samples were easily disaggregated for grain size analysis using a rock crusher. Grain size was measured using a set of nested, wire-mesh screens ranging in size from 2 mm (-1.0Φ very coarse sand) down to 0.063 mm (4.0Φ sand/silt break) (Boggs, 2001). Using cumulative frequency curves (Appendix B) generated from the sorted samples, graphic standard deviations were calculated in order to mathematically determine the sorting of the samples. The calculated standard deviations for each facies sampled are summarized in Table 2. The following equation from Folk and Ward (1957) was used for the calculations:

EQ. 1 $$\sigma_i = ((\Phi_{84} - \Phi_{16})/4) + ((\Phi_{95} - \Phi_5)/6.6),$$

where Φ_{84} means the Φ size at the 84^{th} percentile.

Thin Sections. Thin sections were prepared from all of the different facies. The thin sections were blue epoxy impregnated to show porosity and stained for plagioclase and potassium feldspar to facilitate mineral identification. A 300 point count analysis was completed on each thin section in order to calculate the porosity as a percent, to classify each facies (Fig. 11), and to recognize important petrologic features (provenance classification can be found in Appendix C). The information gathered from these analyses can be found on Table 3.

Table 2. Grain size and sorting of facies associated with eolian-dominated sandstone bodies. Sample *SF-3-SILT did not fully disaggregate due to its high clay content. The thin section of this sample was used to estimate sorting.

Sample	Stand. Dev.	Sorting	Mean Grain Size
SF-3-URL	0.56	mod. well sorted	lower fine
SF-4-URL	0.57	mod. well sorted	lower fine
NF-3-URL	0.63	mod. well sorted	upper fine
NF-1-SDS	0.48	well sorted	lower fine
SF-1-SDS	0.45	well sorted	lower fine
SF-3-LDS	0.63	mod. well sorted	lower fine
SF-4-LDS	0.64	mod. well sorted	lower fine
SF-3-BRL	0.58	mod. well sorted	upper very fine
SF-4-BRLa	0.65	mod. well sorted	upper very fine
SF-3-BCB	0.56	mod. well sorted	upper very fine
SF-1-UNS	0.58	mod. well sorted	upper very fine
SF-3-UNS	0.73	mod. sorted	upper very fine
NF-1-RLC	0.89	mod. sorted	upper fine
*SF-3-SILT		very well sorted	silt

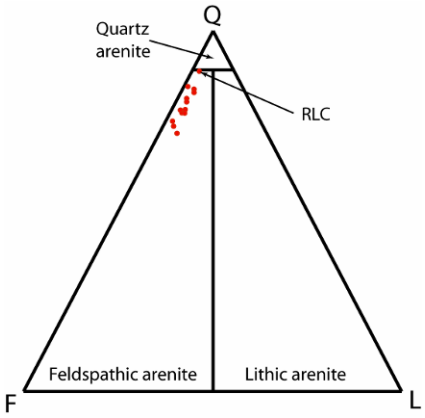

Figure 11. QFL diagram displaying the sandstone classification of the different facies. Modified from Dott (1964).

Core Plug Samples. Core plugs were only extractable from the basal ripple laminated (BRL) facies. Plugs of the BRL facies were analyzed with our TerraTek 8400 Dual Porosimeter/Permeameter. Multiple coring attempts from all other facies failed due to the extreme friability of the sandstones. Many of the sandstones can be pulverized simply by tossing them against a rock. This extreme friability was likely accentuated by weathering. Calcite appeared to be the primary cementing agent in these sandstones yet in most of the facies calcite cement was only 1-7% (Table 3).

Table 3. This table displays the thin section point count values and the machine calculated porosity and permeability values. The thin section porosity values for SF-4-BRLa and NF-1-CS did not correlate with machine calculated values. The reasons for this are: The SF-4-BRLa thin section sampled a portion of the rock that had a thick band of tighter grains (as in the clay-rich bands in Figure 14d) and did not give a good representation of the entire rock sampled. The NF-1-CS point count porosity was lower because the majority of the machine-calculated porosity came from clays which did not show porosity in thin section. The *SF-3-SILT and NF-1-MUD samples were not point counted due to their grain sizes. However, some porosity may be assumed to exist due to their clay content.

	Machine Calculated Values		Thin Section Point Counted Values				
					Normalized QFL		
Sample	Por. (%)	Perm. (mD)	%Por.	%Cal. Cement	%Quartz	%Feldspar	%Lithics
NF-1-MUD	/	/	/	/	/	/	/
SF-3-BCB	/	/	27.0	3.7	77.4	19.2	3.4
SF-3-BRLa	23.9 & 25.5	7.4 & 27.5	23.7	4.3	77.3	18.5	4.2
SF-4-BRLa	25.7	264.2	19.0*	2.3	78.3	17.7	4.0
SF-4-BRLb	/	/	24.3	4.7	74.9	22.8	2.3
NF-1-SDS	/	/	30.7	1.7	80.3	16.2	3.5
SF-1-SDS	/	/	26.3	5.0	81.4	15.7	2.9
SF-3-LDS	/	/	28.3	1.0	84.0	12.7	3.3
SF-4-LDS	/	/	27.7	4.0	84.6	13.9	1.5
SF-4-LDS-CF	/	/	22.0	2.3	78.0	19.2	2.8
SF-4-URL	/	/	26.7	6.3	83.0	13.0	4.0
SF-1-UNS	/	/	25.3	5.0	71.5	23.2	5.3
NF-1-RLC	/	/	18.3	7.3	88.8	8.5	2.7
NF-1-CS	9.3	7.4	3.0*	31.3	73.7	23.2	3.1
*SF-3-SILT	/	/	/	/	/	/	/

Facies Mapping & Descriptions

Figure 12 shows the general facies associations found in both the North and South Fields. Two detailed measured sections also show the exact thickness of each facies along with their relative positions to each other (Fig. 13). Below are detailed descriptions of each facies including data from grain size, thin section, and core plug analyses performed on them.

MUD (Mudstone). Where the very base of the sandstone bodies are exposed, a mudstone facies can be found. Only on five of the twelve sandstone bodies from both the North and South Fields is the base exposed. Below exposed bases a thin muddy facies can often be observed. The mud likely creates a fluid barrier when placed in a subsurface petroleum field environment (Fig. 14a). Below the 3-5 cm thick muddy facies are several silts, dirty sands, and more mudstones which are representative of the tidal flat environment.

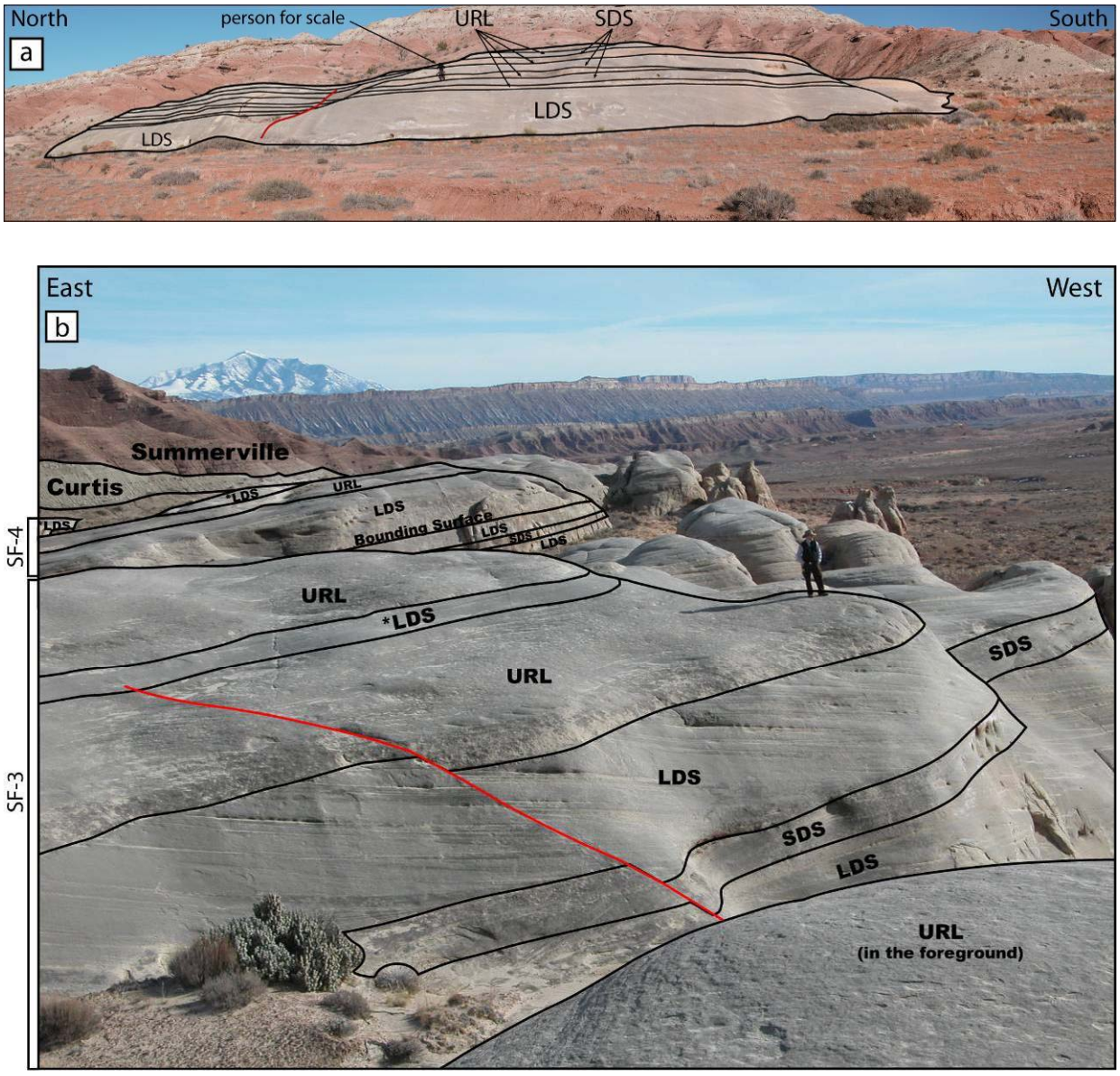

Figure 12. a) Facies relationships commonly found in the North Field with the red line indicating a fault. This photograph is of NF-3. b) Facies relationships commonly found in the South Field. This picture includes SF-3 in the foreground (as well as where the person is standing) and SF-4 in the background. The *LDS represents sections of the LDS facies that were highly scoured.

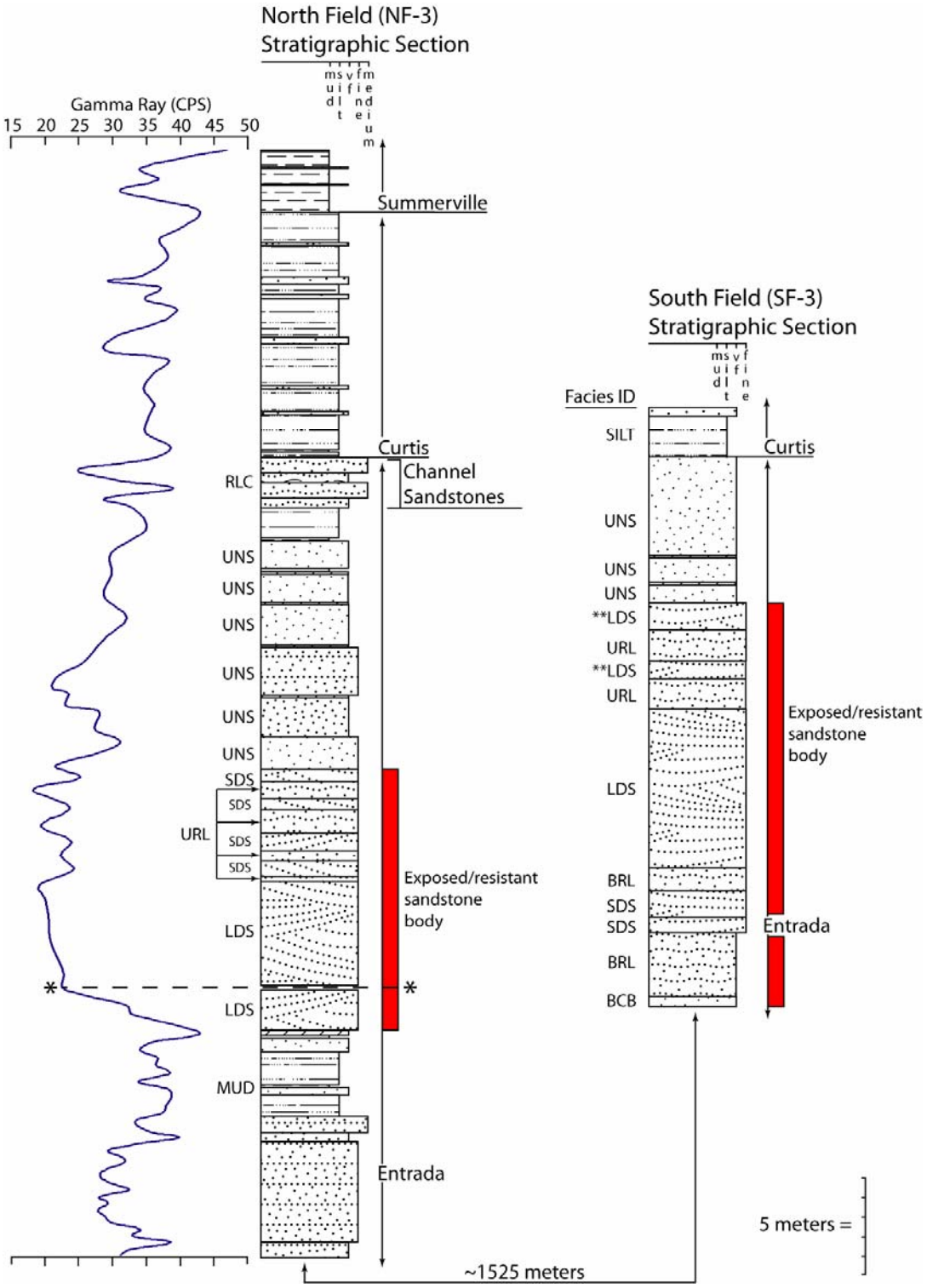

Figure 13. Measured sections and scintillometer measurements of outcrops in the North and South Fields. *Because of the difficulty in finding a portion of the outcrop that exposes the middle, muddier Entrada up through the Summerville, this figure represents a composite measured section. The scintillometer measurements were adjusted accordingly. The section above the dashed line was measured where the Curtis-Summerville contact is exposed while the section below it was taken from an outcrop that displayed the muddy portion of the Entrada. Facies are identified on the left side of both sections. The **LDS represents sections of the LDS facies that were highly scoured.

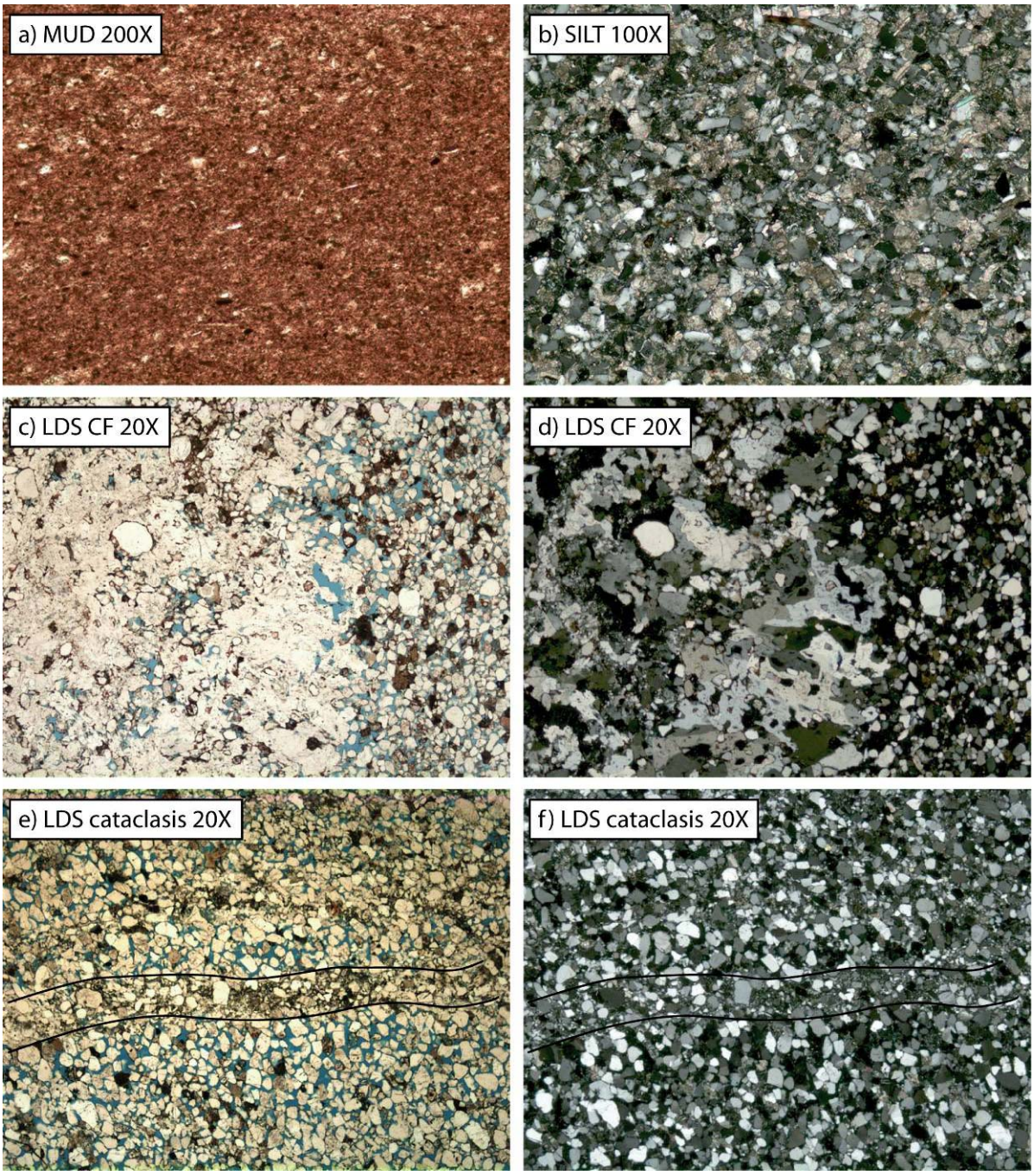

Figure 14. a) Highly magnified mudstone displaying an abundance of clay-sized particles throughout the sample. b) Siltstone showing very little porosity with a high percent of calcite cement. c) Uncrossed and d) crossed polarized view of a fracture fill mineral that has the optical properties of quartz (i.e. uniaxial positive – likely alpha or beta quartz, or even chalcedony). e) Uncrossed and f) crossed polarized view of fractures within the LDS facies where cataclasis occurred. Note the thin band of finely crushed grains.

BCB (Basal Convolute Bedding). At the base of a particularly well exposed sandstone body (SF-3) convolute bedding was abundant. This facies consists of upper very fine sand grains that are moderately well sorted (Table 2). Convolute bedding is a good indicator of rapid deposition and in this situation may have been formed from post-depositional loading (Collinson and Thompson, 1982). The point count porosity for this facies was calculated to be 27%.

BRL (Basal Ripple Laminated). Near the base of three of the six sandstone bodies in the South Field, a facies of asymmetrical ripple lamination and sometimes very small scale trough cross-stratification can be found. If this facies is not at the base it is either directly above the BCB facies or a SDS facies. The BRL facies is very similar to the BCB facies relative to grain size and sorting and is likely what was liquefied and altered to the convolute bedding (Table 2). Thin section work indicates that this facies has high barrier/baffle potential even though it has porosity values ranging from 23.9-25.7%. Within these feldspathic arenite sandstones (Fig. 11) there can be found alternating laminae of more clay-rich sandstone and laminae of less clay-rich sandstone (Fig. 15d). The pore spaces within the clay-rich laminae have clay fibers bridging across pores connecting the grains (Fig. 15f). Of the three point-counted thin sections for this facies, an average of 60% of the overall porosity had clay growing across the pore spaces. Low permeabilities of 7.4 mD up to 264.2 mD reflect how these clay-rich laminae may affect the flow of fluids through this facies. It is likely that the clay in the pore spaces helped to indurate the rock enough as to allow us to extract the core plugs.

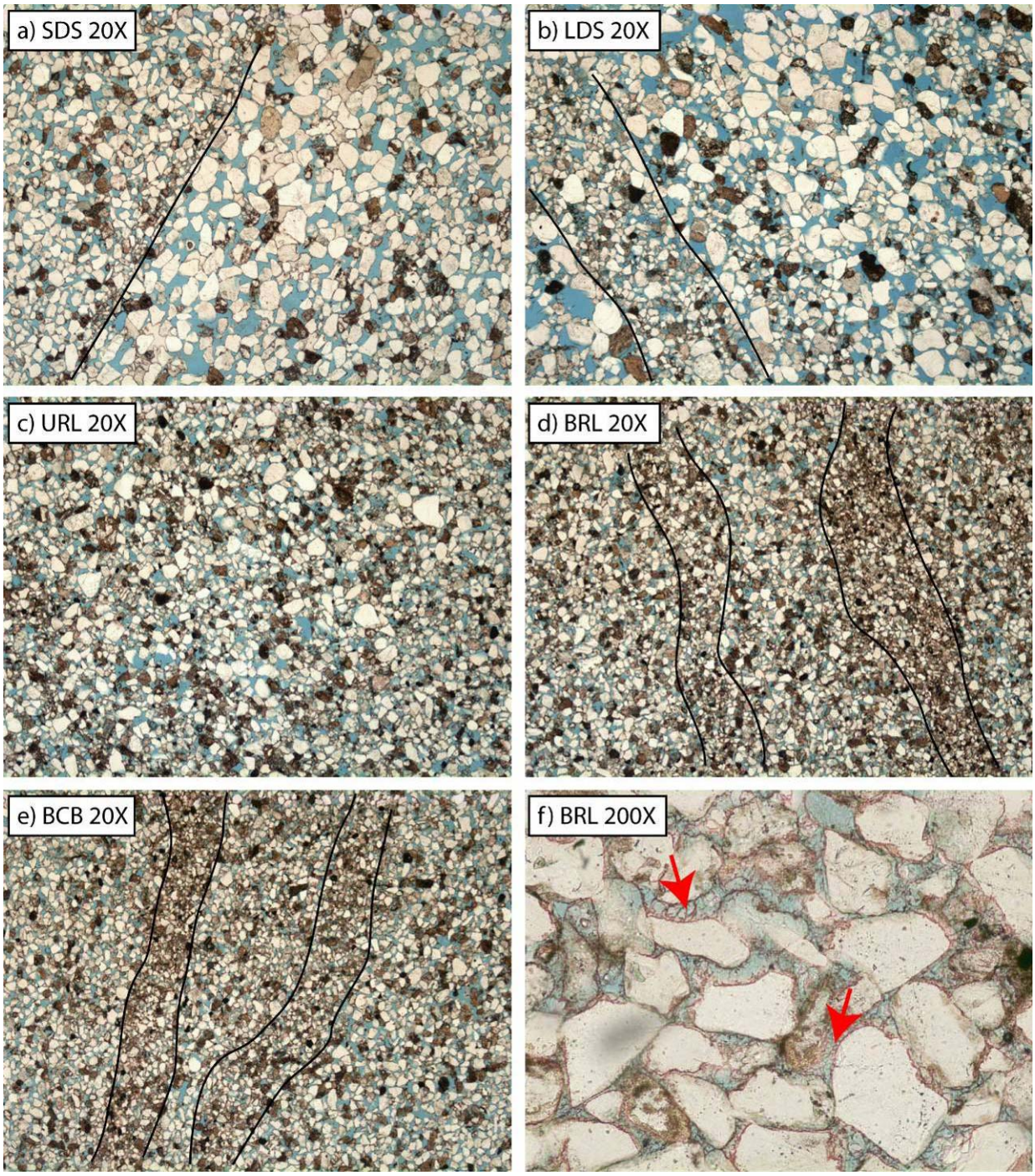

Figure 15. a) and b) SDS and LDS facies respectively, both displaying laminations of relatively coarse and fine sediment from wind blown trough cross-stratification. Note the abundance of well connected pore spaces (blue). c) Reworked sands of the URL facies. Note the grain size and sorting variation from the BRL facies. This is one reason we do not believe these two facies are related. d) BRL sandstone with laminae of finer-grained clay-rich sandstone and larger-grained more porous sandstone. e) BCB facies displaying similar characteristics of the BRL photomicrographs. f) Red arrows point to some of the clay fibers, or "bridges", that are present between the grains in the clay-rich laminae of the BRL facies.

SDS (Small Dune Sets). The small dune set facies can be found towards the base and the top of the sandstone bodies. It consists of smaller dune sets (less than 1 meter) of medium to high angle trough cross-stratified sandstone. These feldspathic arenites have the best sorting of all of the facies (well sorted) and are composed of lower fine grain sand (Fig. 11 & 15a; Table 2). These sandstones give point count porosities of 28-29% and, along with the LDS facies, are the best reservoir quality sandstones found in the outcrop.

LDS (Large Dune Sets). The middle sections of the sandstone bodies are comprised primarily of large dune sets (greater than 1 meter) of medium to high angle trough cross-stratified sandstone. These are moderately well sorted feldspathic arenites. The grain size is lower fine (Fig. 11 & 15b; Table 2). The point count porosities are approximately 28%. Alternating bands of coarser and finer-grained laminae, characteristic of wind blown sands, are readily visible in thin section (Fig. 15b).

URL (Upper Ripple Laminated). The upper ripple laminated sandstone facies can be found towards the top of almost all the sandstone bodies in both the North and South Fields. This sandstone facies is laterally continuous. Its basal contact is scoured but flat. This facies displays climbing ripples, symmetrical ripples, convolute bedding, and bioturbation. The sandstones are moderately well sorted feldspathic arenites composed of upper and lower fine sand (Fig. 11 & 13c; Table 2). Point count porosities ranged around 25%. This facies does not have the clay-rich laminae or the same mean grain size associated with the BRL facies so we do not think they are related. However, the URL facies is very similar to the SDS and LDS facies with respect to its stratigraphic position and mean grain size. This facies likely represents time periods when the water table rose relative to the dunes being deposited. This caused the wind-blown sand to be reworked by water (probably tidal fluxes). There are places where the URL facies is scoured. In

one place the URL facies was completely scoured by migrating dunes of the LDS facies (Fig. 16). These instances probably occurred after the water table fell leaving the newly deposited URL sands time to dry out. When dry, they were susceptible to scouring by migrating eolian dunes.

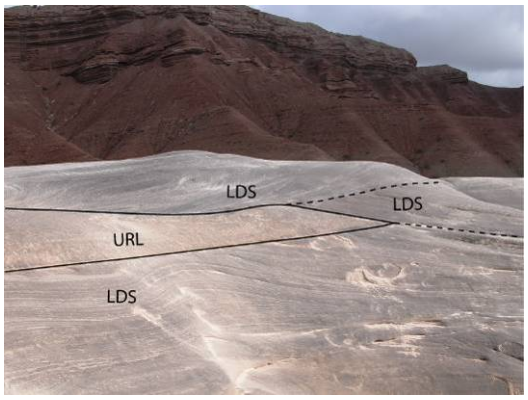

Figure 16. Example where the URL facies is scoured entirely through by the LDS eolian facies.

UNS (Upper Non-resistant Sandstones). Directly above the ledge-forming bleached sandstone bodies, less resistant sandstones are present. These sandstones form slopes similar to the muddy, Curtis siltstones. They are moderate to moderately-well sorted feldspathic arenites. They are composed of primarily upper very fine sand rather than fine sand like most of the previous sandy facies (Fig. 11 & 17a; Table 2). This grain size difference is likely one of the factors that allow these sandstones to be less resistant than others. The point count porosities ranged around 25% yet; this facies has thick laminations of almost silt-sized grains that would likely reduce permeability (Fig. 17a).

RLC (Ripple Laminated Channel). A facies of channel sandstones can be found at the top of few of the Entrada sections in the North Field, just below the Curtis Formation (Fig. 18). These sandstones are more coarse (upper fine) than the other facies. The point count porosity in this facies drops to 18% and the percent of calcite cement rises to 7.3% (Table 3). The classification of the RLC sandstones fell on the border between a quartz arenite and a feldspathic arenite (Fig. 11). This facies contains two things that no other facies does which are quartz overgrowths and rip-up clasts, both of which are visible in thin section (Fig. 17b). These channel sandstones can be found in association with tidal flat deposits and are in direct communication with the eolian-dominated sandstones.

SILT (Siltstone). The last facies identified was the lower siltstone of the Curtis Formation. The SILT facies exhibited no visual porosity and likely acts as a significant barrier to the Entrada sandstones below (Fig. 14b).

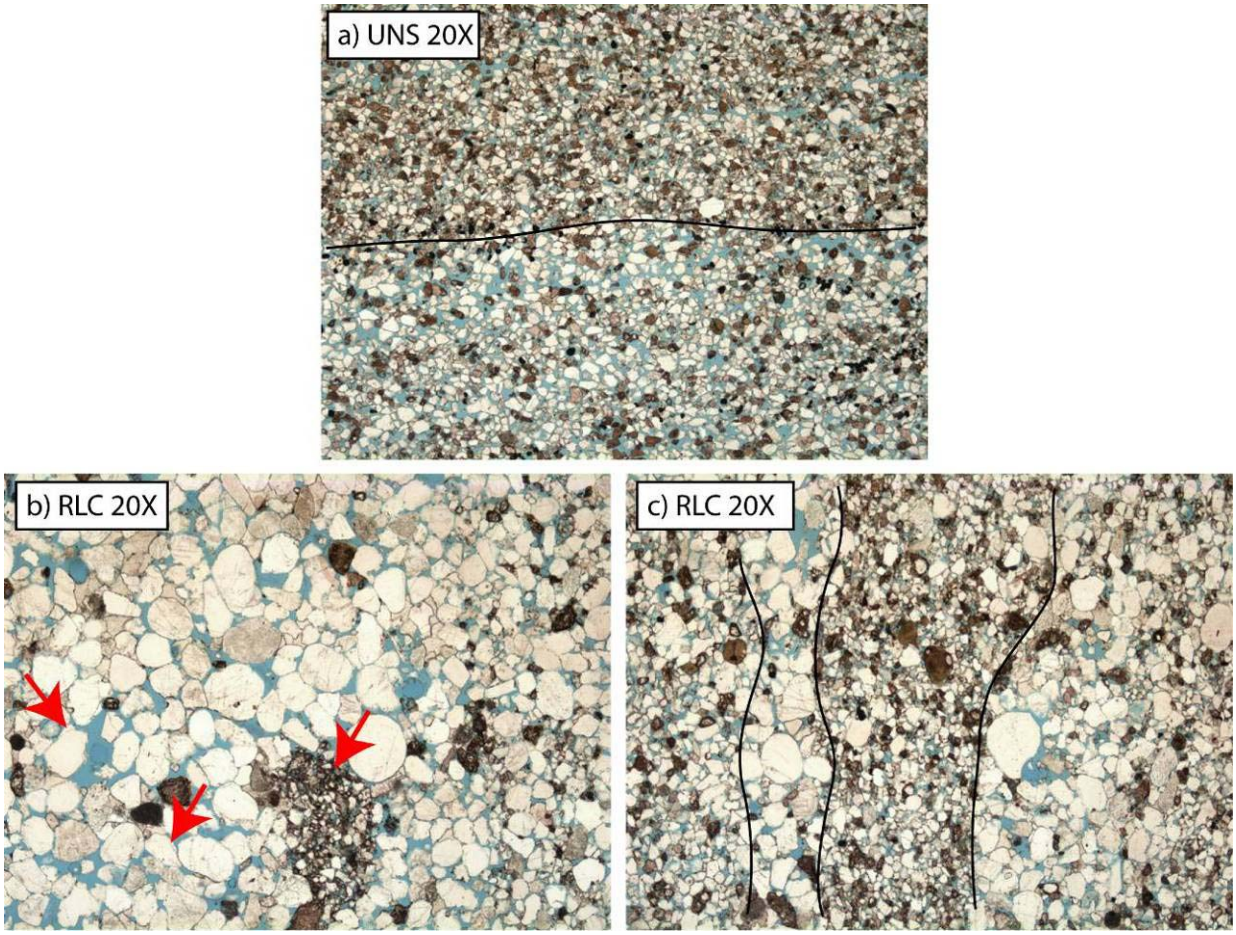

Figure 17. a) Upper very fine-grained UNS facies displaying banding of the coarse and fine grains. b) & c) RLC facies showing a much larger grain size (upper fine) along with a rip-up clast and quartz overgrowths. The red arrows indicate the quartz overgrowths and the rip-up clast. Finer-grained laminations are also present in the RLC faices and can be seen in c).

Figure 18. Channel sandstones directly above NF-3 that are interpreted to be correlative to channel sandstones directly on top of NF-1 eolian sandstones. There is a person and a 1.5 m jacob staff for scale.

Well Logs

Well Log Analysis. The NHC/FR field well logs (Fig. 19) show that Entrada sandstones are sealed on the top and bottom by the mudstones of the Curtis and Carmel Formations, respectively. Interesting, the NHC/FR field is producing gas in only certain sections of the Entrada Sandstone. By looking at the gas crossover effect displayed in Figure 19, compartmentalization of the gas-bearing zones is readily notable. It is this relationship, along with the amplitude time slice viewing of 3D seismic data (Eckels et al., 2005) in the NHC/FR field and previous studies that initiated the idea that the productive Entrada sandstones were coastal erg-margin deposits (Mariño and Morris, 1996; Marc Eckels, personal communication 2005).

It is notable that while Log 2 has gas crossover almost throughout the entire Entrada section, Log 3 only has crossover in two smaller zones. The GR curves of Log 2 appear much sandier relative to Log 3. Log 3 represents a section with more mudstones and reworked sandstones which would allow for greater compartmentalization of the gas-bearing zones. The variation throughout these well logs is likely due to their relative position in the erg-margin

(whether it is more seaward or landward). The Entrada sections of the case study are best correlated with Log 3, due to the relative muddiness of this well log (see below).

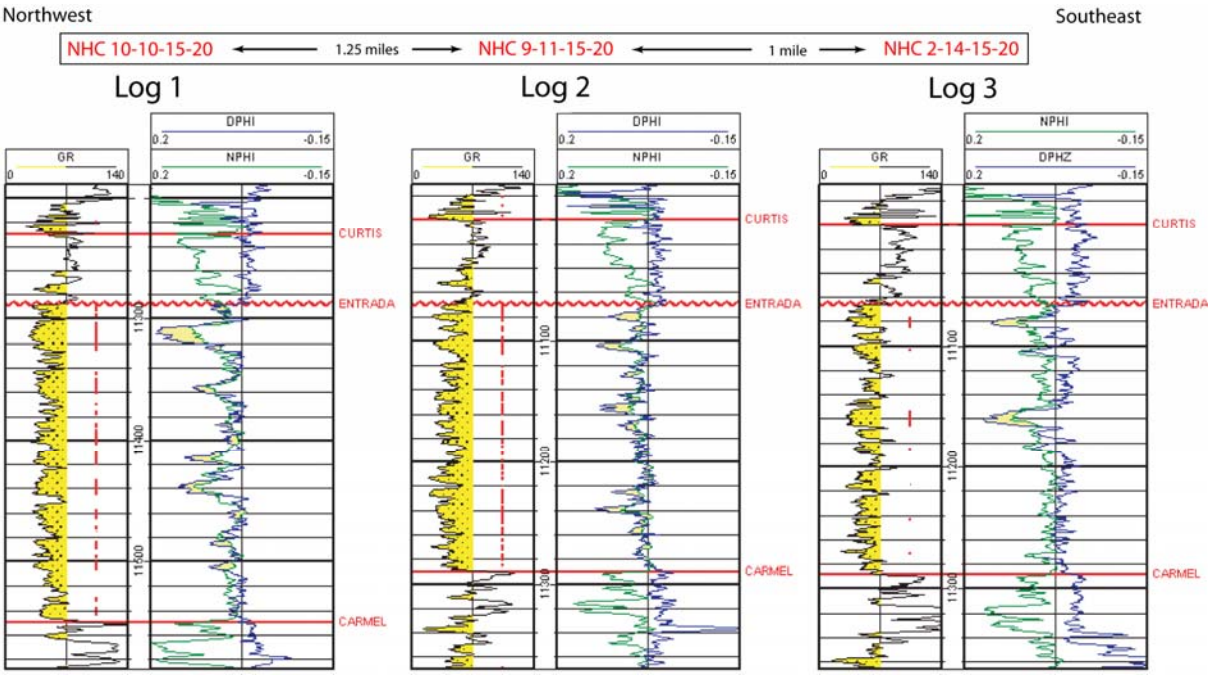

Figure 19. Three well logs from the NHC/FR field that display the entire Entrada section. The logs are hung from the top of the Entrada Sandstone. To better display the muddier intertidal sections on the well logs, all zones between the 70 CPS line and the GR curve were shaded yellow with a sandstone pattern. Neutron and Density Porosity curves were plotted and shaded where they cross to highlight the gas effect. To aid correlation, all gas effect zones were plotted as the vertical red lines to the right of the GR curve seen in Track 1.

Outcrop Scintillometer Curves & Log Correlation. In order to compare data to the NHC/FR field well logs, we created our own gamma ray curves along the Entrada sections exposed at the case study area. Scintillometer (gamma ray) readings were taken at approximately 1.5 ft intervals along the same sections of outcrop used for detailed measured sections. These scintillometer readings were plotted as curves and tied to the measured sections (Fig. 20). The curves that were generated from this sampling display positive and negative GR kicks within the Entrada (with positive kicks occurring between the eolian sandstone bodies). The Curtis Formation generally displays a fining upward trend on the GR curve though several thin sandstone stringers do give some negative kicks.

Good correlation exists between the generated scintillometer curve and the NHC/FR field well logs. The well logs in the NHC/FR field show a consistent fining upward pattern merging from the top of the Entrada up through the Curtis Formation. As mentioned previously, this pattern is also visible in our scintillometer curve (Figs. 13 & 20).

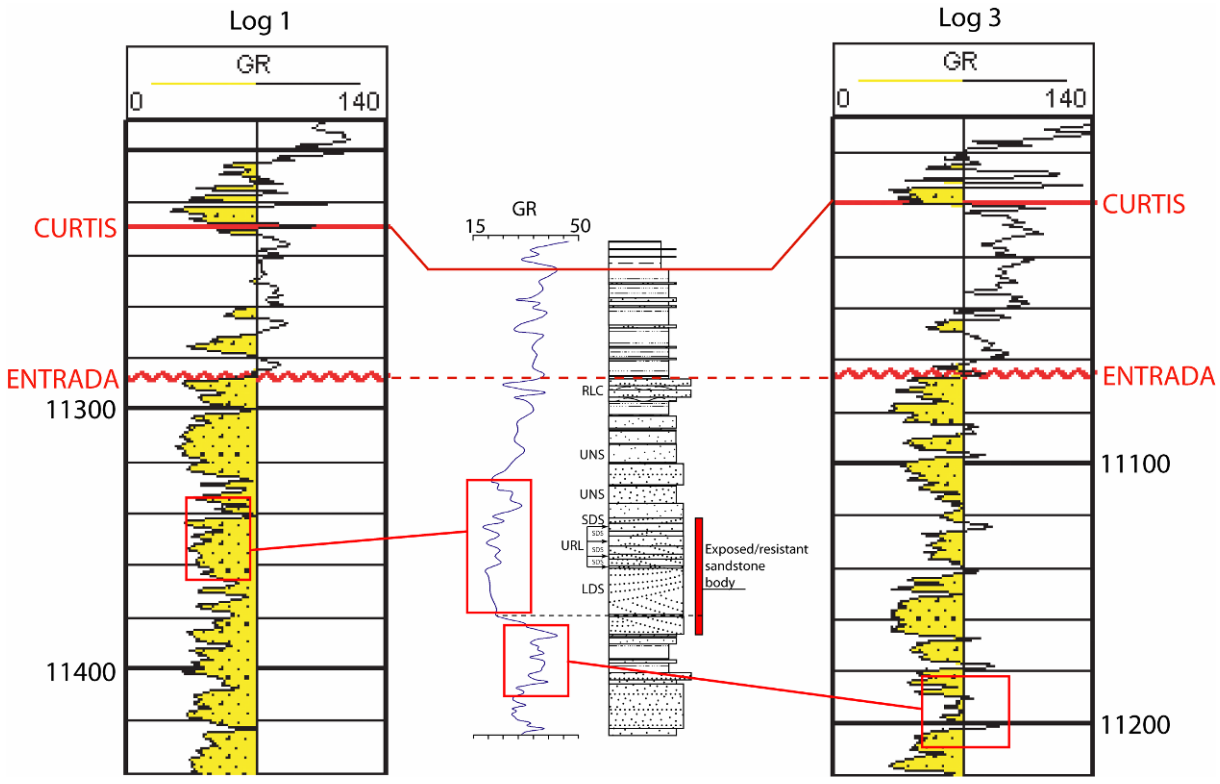

Figure 20. Two well logs are compared to our generated GR curve. All of the curves are hung from the top of the Entrada. The connected red boxes show similar response areas of the well logs and scintillometer curve. The measured section and scintillometer curve are scaled to fit to the well logs which are scaled in feet.

An apparent difference between the scintillometer curve and Log 1 was the large positive kicks found in the Entrada section of the outcrop. Log 1 does not display such large positive kicks. However, other well logs, especially Log 3, do show large positive kicks. For example, the positive kicks from 11190 to 11200 ft on Log 3 could represent a muddier section very similar to the ones found in outcrop. Further, there are several smaller kicks in the well logs that mimic the GR responses we found across the alternating beds of URL and UNS sandstones (both reworked) and cleaner trough cross-bedded sandstones (Fig. 20). We believe most of the

positive kicks in Logs 1 and 2 were produced by reworked sandstones that accumulated some muddy ripple lamination rather than mudstone-dominated stratal units of the Entrada. The variation found in the well logs and the scintillometer curve is attributed to the relative location of the outcrop verses the NHC/FR field within the coastal erg-margin.

Because the well logs appear to be more sandy (with fewer positive kicks) relative to the case study outcrop, we believe they represent a location in the coastal erg-margin that is closer to the erg proper. We expect that the case study outcrop represents a more seaward position on the erg-margin where finer silts and muds can be deposited. This relationship is visible in Figure 2 (erg-margin map) with the NHC/FR field being located on the eastern edge of the erg-margin and our case study area towards the center. We speculate that because of the NHC/FR field's close proximity to the body of the erg, it had more sand supply. Tidal fluctuations caused reworking of these clean eolian sands resulting in relatively sand-rich facies (rather than more silt and mud-rich facies). Even with decreased mud and silt intermixed with the sandstones of NHC/FR field, there could still be significant barriers and baffles throughout the Entrada section that would cause compartmentalization of gas. In fact, even within eolian-dominated sandstones, water deposited ripple lamination may produce positive GR kicks that can serve as potential baffles to fluid flow. For example, some of the BRL facies have permeabilities as low as 7.4 mD which would be more than adequate to produce a significant baffle or barrier relative to the ambient facies.

Porosities were calculated for the Entrada Sandstone from the NHC/FR field well logs. Density porosity well logs, as well as the volume of shale (V_{shale}) in the zone of interest, were used to calculate the *effective* porosities of these sandstones. The procedure and necessary

equations used in this process are outlined in *Basic Well Log Analysis* by Asquith and Krygowski (2004).

The majority of the Entrada sandstones analyzed from the well logs have low porosities ranging around 4%. However, the better reservoir quality zones of Log 2 have 10.2-12.9% porosities while those of Log 3 have 14.8-16.1% porosities. The values we calculated are significantly less than those found from sample analyses of the case study outcrop. We attribute this variation partly to cement reduction from weathering.

Barriers

Vertical barriers probably do not exist within the eolian-dominated sandstone bodies of the case study area. Although at least nine facies are recognized within and associated to the eolian-dominated sandstone bodies, the vertical succession of these facies produces no barrier to fluid flow within the reservoir. Enveloping mudstones, stratigraphically above and below the sandstone bodies, act as seals (Fig. 21a). In some instances eolian-dominated Entrada sandstone bodies may be in communication with the thin sandstones of the Curtis Formation, but the Curtis sandstone that was sampled gave a relatively low permeability of 1.5 mD (Table 3). The Curtis is overlain by sealing mudstones of the Summerville Formation.

Lateral barriers exist at the edges of the eolian-dominated sandstone "fields" as the sandstones inevitably pinchout into tidal flat mudstones and siltstones. However, this may not happen immediately at the edge of the eolian-dominated sandstones as there is some evidence that tide-reworked sandstones exist lateral to the eolian-dominated sandstones. These tidal-influenced sandstones are relatively thin but can be laterally extensive (0.5 km or more). Thin

channel-form sandstones associated within the tidal flat may also be in communication with the eolian-dominated sandstones (Fig. 18).

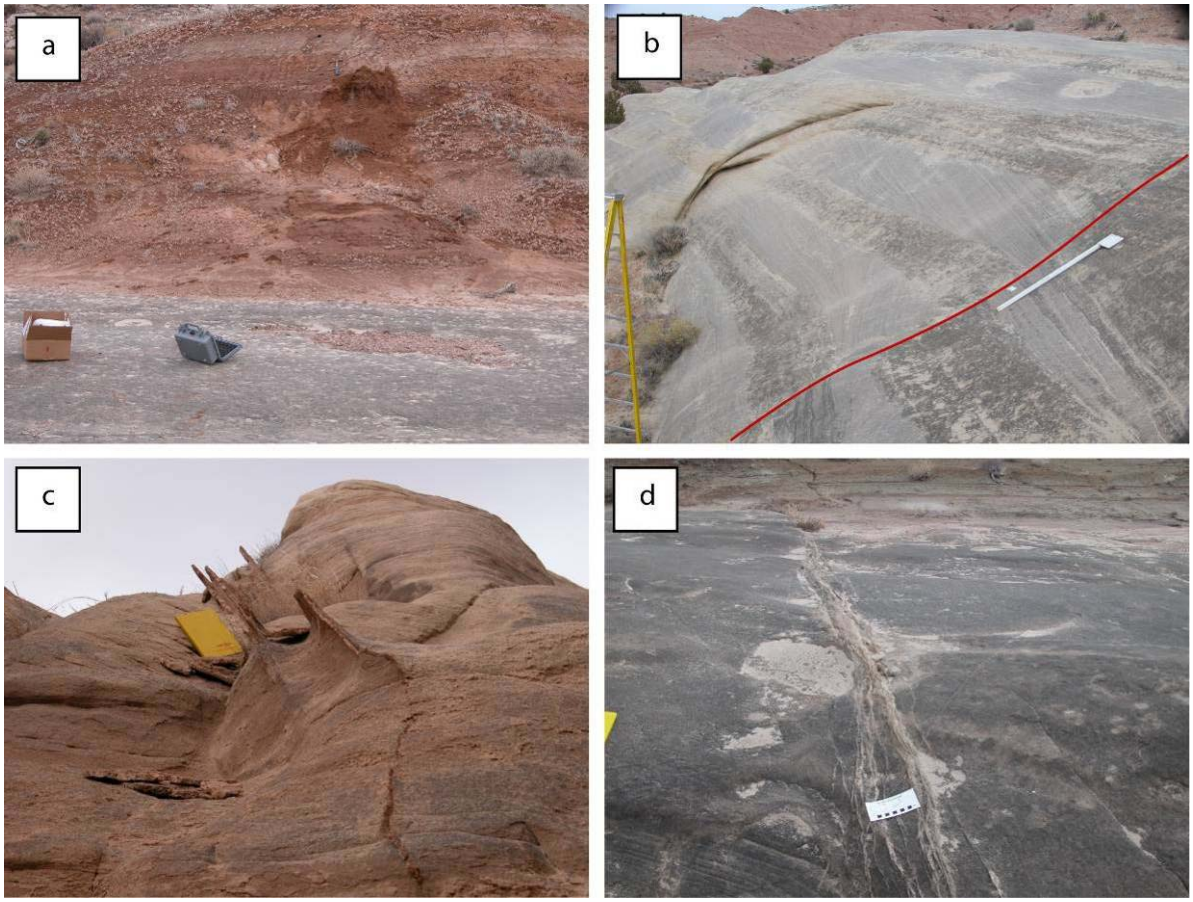

Figure 21. a) Entrada mudstones overlying Entrada reservoir quality, eolian-dominated sandstones. b) A fault with less than one meter of vertical displacement in sandstone body NF-2. Note the lack of differential relief along the fault plane. 1.5 m jacob staff for scale. c) Differential relief along the quartz-cemented fracture fill in sandstone body SF-3. d) Fracture/fault swarm exhibiting only moderate relief. Shearing along these fractures has caused the grains to undergo cataclasis leaving thin bands of much finer grains (Fig. 14e and f). The throw on the faults are on the order of a few centimeters.

Baffles

Faults. High angle faults exist in the field study sandstones but they have minimal throw (1 meter or less) (Fig. 21b). Based on the lack of differential weathering in the damage zone, and close investigation of the outcrop, there appears to be a sandstone to sandstone contact with no preferred cementation. However, this is not true of many fracture fills (see below) which leave

open the possibility that cementation in fault damage zones could potentially baffle or prevent (barrier) fluid communication across faults.

Fractures. We have observed at least one fracture that is preferentially cemented with quartz (Fig. 21c). In outcrop the quartz-filled fractures stand out in relief relative to the sandstone body. The quartz classification is based on the optical properties of the cement as seen in thin section (Fig. 14c & d). In thin section it is obvious that the porosity is reduced but not obliterated. Since we were unable to extract a core plug across the fracture fill, the permeability is unknown. Our experience, however, tells us that permeability would be dramatically reduced across the fracture therefore, at a minimum, these types of features likely act as significant baffles to liquid hydrocarbons and possibly to natural gas.

There are many fracture swarms that exhibit moderate relief from the outcrop. In these fractures the grains have undergone cataclasis, creating thin bands of silt-sized particles (Figs. 21d, 14e & f). These bands undoubtedly act as fluid baffles due to the sudden decrease in grain size.

Facies and Bounding Surfaces. Baffles probably do exist within the eolian-dominated sandstone bodies especially when the upper rippled laminated facies is present. The contact between this facies and those below represents a first-order bounding surface, which likely acts as a significant baffle (Boggs, 2001). The basal rippled laminated facies displays the lowest permeability within the bodies (varying between bodies 7.4 - 27.5 - 264.2 mD). This reduction in permeability can be attributed to the clay-rich laminae found in the thin sections of this facies (as explained in the BRL facies description).

The facies bounding surface work of Mayo et al. (2003), Holman (2001), and Black (2000) demonstrates that permeability across a facies contact is generally lower than the ambient

permeability in either of the facies above or below the contact. One would expect significant drop in permeability across the contact of two facies even though neither facies is impermeable. Therefore, laterally extensive, horizontal facies contacts may act as baffles to flow. The baffling effect would be more pronounced in reservoirs filled with liquid hydrocarbons than those charged with natural gas.

SUMMARY

- The Entrada erg-margin can be located in outcrop and subcrop within the State of Utah. Literature reviews, surface reconnaissance, and well bore penetrations have been used to outline the erg-margin trend.
- Because the Entrada erg-margin has high potential to develop stratigraphic and combination traps, subcropping areas are prospective for future gas exploitation.
- The case study area represents a good outcrop analog to the NHC/FR field although we interpret the case study area to be located in the central portion of the erg-margin whereas the NHC/FR field is located nearer the erg proper.

CONCLUSIONS

Numerous critical conclusions can be drawn from this study. Each conclusion can be categorized into the following areas: Sedimentology and Stratigraphy, Seismic Geophysics, and Petrology and Reservoir Quality. We herein list the major conclusions in each of these areas. In the final section of the report we discuss suggested practices that relate directly to our conclusions. These conclusions and suggested practices are intended to aid further exploitation of the Entrada erg-margin play in the State of Utah.

Sedimentology and Stratigraphy

- There are nine recognizable facies within or directly associated with the eolian-dominated reservoir quality sandstone bodies of the upper Entrada Sandstone in the case study area. Reservoir quality facies in order from highest to lowest include: small dune set (SDS), large dune set (LDS), and upper ripple laminated (URL). Volumetrically, these three facies constitute over 70% of the sandstone bodies. Intermediate reservoir quality facies that may serve as baffles both above and below the high quality reservoir facies include: basal ripple laminated (BRL), basal convolute bedding (BCB), and siltsones (SILT). BRL and BCB facies are found directly below the reservoir quality sandstone bodies whereas siltstone can be found both above and below the sandstone bodies. A non-reservoir quality facies that serves as a seal to the reservoir quality sandstone bodies is the Mudstone facies (MUD). This facies is found above, below, and eventually lateral to the sandstone bodies.
- Individual sandstones bodies in the case study area can be grouped into "fields" (i.e the North Field and the South Field). Sandstone bodies within these fields are often genetically related. Most of the sandstone bodies within a given field are in communication with other sandstone bodies within that field. The two fields of the case study area are interpreted to be isolated from each other.
- Dune complexes migrate southward through time. They are diachronous in nature. They should not be expected to be found at the same stratigraphic level even within a given "field".

- There can be significant differences (ten's of meters) in the stratgraphic thickness of the Curtis Formation in the field study area. This variation is undoubtedly related to the uncomformity between the Curtis Formation and the Entrada Sandstone.
- Measured sections and stratigraphic correlation suggest a relationship between a sandstone body's thickness and its probability of being associated with a large dune complex. Sandstone bodies with thicknesses of greater than 10 m are all associated to a dune complex that is interpreted to be in reservoir communication. Sandstone bodies less than 10 m have only a 40% chance of being associated with a dune complex.

Seismic Geophysics

- On the high resolution shallow seismic lines shot in the field study area, the eolian-dominated reservoir quality sandstone bodies of the upper Entrada Sandstone are interpreted to be resolvable and appear at the exact depth expected from measured sections in outcrop.
- Entrada sandstone bodies contain no resolvable internal reflectors and appear to scatter and attenuate the remaining seismic energy beneath them.
- Gypsum-filled fault gouge causes seismic washout in the near fault area.
- Boulder-filled pediment channels can create near surface seismic attenuation.
- Small-scale faults and fractures observed in seismic and from outcrop within the Summerville Formation suggest that compressional stress occurring in post Summerville time may have reacted to relatively thick sandstones of the upper Entrada Sandstone. It appears that the sandstone bodies acted as more coherent

blocks. Thus, the compressional stress was absorbed in the Summerville creating the abundance of fractures and small-scale faults observed.

Petrology and Reservoir Quality

- The Small Dune Set (SDS) and Large Dune Set (LDS) facies display the best combined porosity and permeability characteristics within the reservoir quality sandstone bodies of the Entrada Sandstone. Both of these facies display eolian deposited characteristics of alternating laminae of finer-grained (upper very fine sand) and coarser-grained (upper fine sand) sand.
- Other than stratigraphic baffles, outcrop and thin section analyses indicate that two additional types of fault/fracture baffles exist within the reservoir quality sandstone bodies. Silica-cemented fractures appear to be significant baffles in the outcrop. Although this fracture fill type is not abundant, thin section analysis indicates significant porosity and permeability reduction. The second type of baffling occurs along small faults in the form of cataclasis. Grain crushing has reduced grain size and therefore permeability. We estimate that this second type of baffle is less effective than the silica-cemented fracture-fill type.
- A 3D seismic survey shot in the NHC/FR field suggests that large dune complexes are composed of migrating star dunes and that smaller sandstone bodies are barcanoid and linear/seif dunes. These features are visible in a modern analog located in the Namibia Desert, Africa.

Suggested Practices

- Suggested Practice - General: As one approaches the erg proper, the reservoir quality and volumes increase but the stratigraphic trap potential may decease. This potential trade-off must be considered in developing an exploration strategy.
- Suggested Practice – Sedimentology and Stratigraphy: The diachronous nature of migrating dune complexes needs to be understood when mapping upper Entrada sandstone reservoirs. Whether mapping from log picks or from seismic picks, one must account for the relative change in the stratigraphic position of migrating dune complexes.
- Suggested Practice – Sedimentology and Stratigraphy: Thickness variation of the Curtis Formation must be understood when mapping the Curtis Formation/Entrada Sandstone contact.
- Suggested Practices – Seismic Geophysics: Gas field development strategies within the Entrada erg-margin gas play should consider the implications of the features observed from the 2D high resolution seismic surveys conducted in this study. Subtle features observed from this study may not be observable on exploration scale seismic, yet may have significant consequences in field development.
- Suggested Practice – Petrology and Reservoir Quality: Well bore completion strategies should consider perforating perpendicular to foreset laminae in an effort to expose as many course-grained laminae to the well bore as possible. These coarser-grained laminae possess relatively high porosity and permeability and would thereby maximize production rates.

- Suggested Practice – Petrology and Reservoir Quality: NHC/FR field development strategy has utilized "frac jobs" in their Entrada completions. Significant improvements have been made from initial production rates upon completion of a frac job (Marc Eckels, Wind River Resources, personal communication). Induced fractures probably reduce or eliminate baffles and barriers in the near well bore area.

ACKNOWLEDGMENTS

This study was funded primarily by the Utah State Geological Survey, Contract # 051844 under the "Characterization of Utah's Natural Gas Reservoirs and Potential New Reserves" Program, for which we are most grateful. Additional funding was received from the College of Physical and Mathematical Sciences at Brigham Young University. We thank Marc Eckels (VP of Wind River Resources) for his willingness to provide us with well logs as well as other information. Processing and visualization software were donated by Haliburton - Landmark ProMAX2D and Seismic Microtechnology's Kingdom Suite.

REFERENCES

Cited

Asquith, G., and D. Krygowski, 2004, Log Interpretation. In: G. Asquith and D. Krygowski, Basic Well Log Analysis. AAPG Methods in Exploration 16, p.115-135.

Black, B.J., 2000, Fluid flow characterization of the Castlegate Sandstone, southern Wasatch Plateau, Utah: Interpretation of reservoir partitioning though permeability and porosity analysis, M.S. thesis, Brigham Young University, 145 p.

Blakey, R.C., 1988, Basin tectonics and erg response. In: G. Kocurek (Editor), Late Paleozoic and Mesozoic Eolian Deposits of the Western Interior of the United States. Sedimentary Geology, v. 56, p. 127-151.

Boggs, S., Jr., 2001, Principles of Sedimentology and Stratigraphy, 3rd ed.: Prentice Hall, Upper Saddle River, 726 p.

Chan, M.A., 1989, Erg margin of the Permian White Rim Sandstone, SE Utah: Sedimentology, v. 36, p. 235-251.

Collinson, J.D., and Thompson, D.B., 1982, Sedimentary Structures: George Allen & Unwin Ltd, London, 194 p.
Dickinson, W.R., 1985, Interpreting provenance relations from detrital modes of sandstones. In: G.G. Zuffa (Editor), Provenance of Arenites. Reidel, Dordrecht, p. 333-361.
Dobrin, M.B., and Savit, C.H., 1988, Introduction to Geophysical Prospecting, 4th ed, McGraw-Hill Book Co., New York City, 867p.
Dott, R.H., 1964, Wacke, greywacke and matrix - what approach to immature sandstone classification?: Journal of Sedimentary Petrology, v. 34, p. 625-632.
Eckels, M.T., Suek, D.H., and Harrison, P.J., 2005, New, old plays in southern Uinta basin get fresh look with 3D seismic technology: Oil & Gas Journal, v. 103, p. 32-40.
Eschner, T.B., and Kocurek, G., 1986, Marine destruction of eolian sand seas; origin of mass flows: Journal of Sedimentary Petrology, v. 56, p. 401-411.
Eschner, T.B., and Kocureck, G.,1988, Origins of relief along contacts between eolian sandstones and overlying marine strata, In: AAPG Bulletin, v. 72, p. 932-943.
Folk, R.L., and Ward, W.C., 1957, Brazos River bar: A study of the significance of grain-size parameters: Journal of Sedimentary Petrology, v. 27, p. 3-26.
Fryberger, S.G., 1986, Stratigraphic traps for petroleum wind-laid rocks: AAPG Bulletin, v. 70, p. 1765-1776.
Holman, L.S., 2001, The effect of parasequence geometry and facies architecture on reservoir partitioning of the Star Point Sandstone, Wasatch Plateau, Utah, M.S. thesis, Brigham Young University, 157 p.
Kocurek, G., 1981, Erg reconstruction: the Entrada Sandstone (Jurassic) of northern Utah and Colorado: Palaeogeography, Palaeoclimatology, Palaeoecology, v. 36, p. 125-153.
Mariño, J.E. and Morris, T.H., 1996, Erg margin and marginal marine facies analysis of the Entrada Sandstone, Utah: Implications to depositional models and hydrocarbon entrapment. In: M. Morales (Editor), The Continental Jurassic. Museum of Northern Arizona Bulletin 60, p. 483-496.
Mayo, A.L., Morris, T.H., Peltier, S., Petersen, E.C., Payne, K., Holman, L. S., Tingey, D., Fogel, T., Black, B. J., and Gibbs, T.D., 2003, Active and in active groundwater flow systems: evidence from stratified mountainous terrain, Geological Society of America Bulletin, v. 115, no. 12, p. 1456-1472.
Peterson, F., 1988, Pennsylvanian to Jurassic eolian transportation systems in the Western United States. In: G. Kocurek (Editor), Late Paleozoic and Mesozoic Eolian Deposits of the Western Interior of the United States. Sedimentary Geology, v. 56, p. 207-260.

Non-cited

Antonellini, M., and Aydin, A.,1994, Effect of faulting on fluid flow in porous sandstones; petrophysical properties, AAPG Bulletin, v. 78, p. 355-377.
Blakey, R.C., Peterson, F., and Kocurek, G., 1988, Synthesis of late Paleozoic and Mesozoic eolian deposits of the Western Interior of the United States. In: G. Kocurek (Editor), Late Paleozoic and Mesozoic Eolian Deposits of the Western Interior of the United States. Sedimentary Geology, v. 56, p. 3-125.
Chan, M.A., and Kocureck, G., 1988, Complexities in eolian and marine interactions; processes and eustatic controls on erg development. In: G. Kocurek (Editor), Late Paleozoic and

Mesozoic Eolian Deposits of the Western Interior of the United States. Sedimentary Geology, v. 56, p. 283-300.
Chan, M.A., Parry, W.T., and Bowman, J.R., 2000, Diagenetic hematite and manganese oxides and fault-related fluid flow in Jurassic sandstones, southeastern Utah, AAPG Bulletin, v. 84, p. 1281-1310.
Doeling, H.H., 2000, Geology of Arches National Park, Grand County, Utah, *in* D.A. Sprinkel, T.C. Chidsey, Jr., and P.B. Anderson, eds., Geology of Utah's Parks and Monuments: Utah Geological Association Publication 28, p. 11-36.
Johansen, S. J., 1988, Origins of upper Paleozoic quartzose sandstones, American Southwest: Sedimentary Geology, v. 56, p. 153-156.
Kocurek, G, 1988, First-order and super bounding surfaces in eolian sequences; bounding surfaces revisited. In: G. Kocurek (Editor), Late Paleozoic and Mesozoic Eolian Deposits of the Western Interior of the United States. Sedimentary Geology, v. 56, p. 193-206.
Kocurek, G., 1991, Eolian event stratigraphy; a conceptual framework: AAPG Bulletin, v. 75, p. 612.
Marzolf, J.E., 1988, Controls on late Paleozoic and early Mesozoic eolian deposition of the Western United States. In: G. Kocurek (Editor), Late Paleozoic and Mesozoic Eolian Deposits of the Western Interior of the United States. Sedimentary Geology, v. 56, p.167-191.
Morris, T.H., Manning, V.W., and Ritter, S.M., 2000, Geology of Capitol Reef National Park, Utah, *in* D.A. Sprinkel, T.C. Chidsey, Jr., and P.B. Anderson, eds., Geology of Utah's Parks and Monuments: Utah Geological Association Publication 28, p. 85-105.
Orhan, H., 1988, Diagenesis of the Entrada Sandstone in Ghost Ranch Area, New Mexico: AAPG Bulletin, v. 72, p. 969.
Reese, R.S., 1981, Stratigraphy and petroleum trapping mechanisms of Upper Jurassic Entrada Sandstone, northwestern New Mexico: AAPG Bulletin, v. 65, p. 567.
Ver Hoeve, M.W., 1982, Facies-controlled diagenesis and reservoir character, Entrada Sandstone (Late Jurassic), Durango, Colorado: AAPG Bulletin, v. 66, p. 638-639.
Vincelette, R.R., and Chittum, W.E., 1981, Exploration for oil accumulations in Entrada Sandstone, San Juan Basin, New Mexico: AAPG Bulletin, v. 65, p. 2546-2570.

APPENDICIES

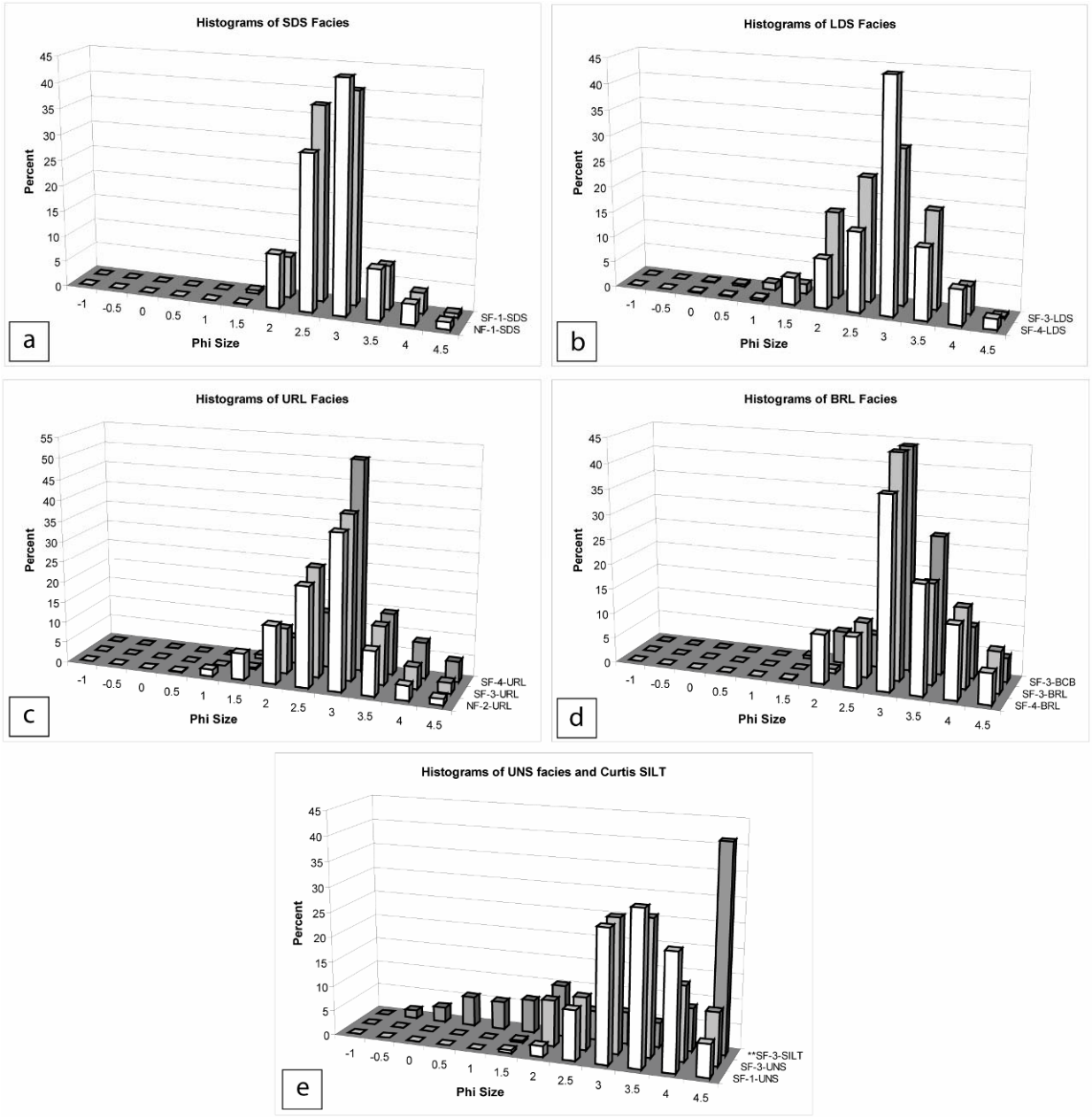

Appendix A. a-e) Histograms of the various facies sampled from multiple locations over both fields. All of the facies produce negatively (coarse) skewed histograms. The 4.5 phi bin of the histograms represents all grains smaller than very fine sand. **The SF-3-SILT sample was poorly sieved due to caked grains that would not break down. From thin section it is obvious that all of the grains fall into the 4.5 phi bin of the histogram.

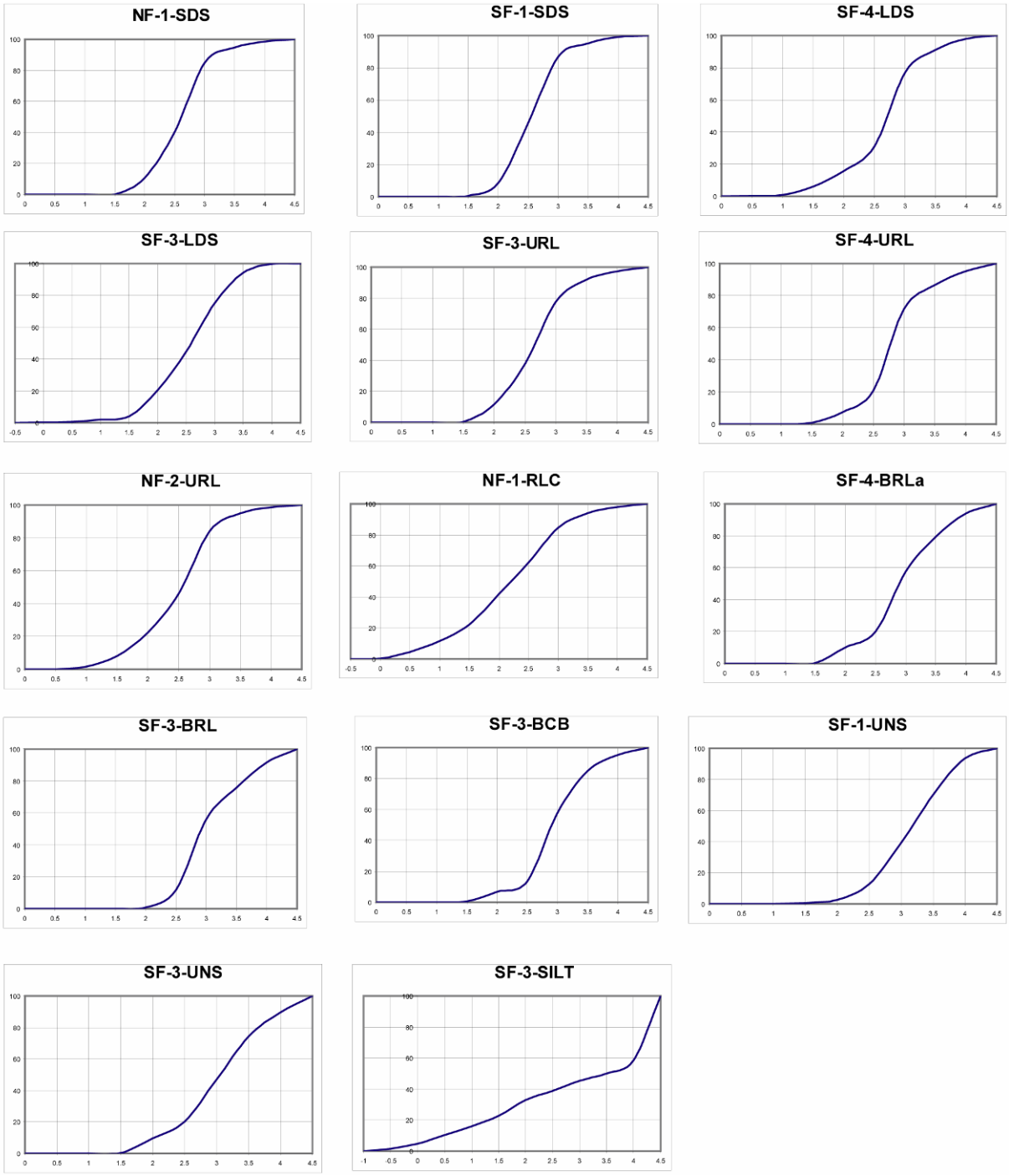

Appendix B. Cumulative frequency curves for all facies. These curves were used for calculating the sorting of the samples. The horizontal scale is grain size in Φ units. The vertical scale is cumulative weight percent.

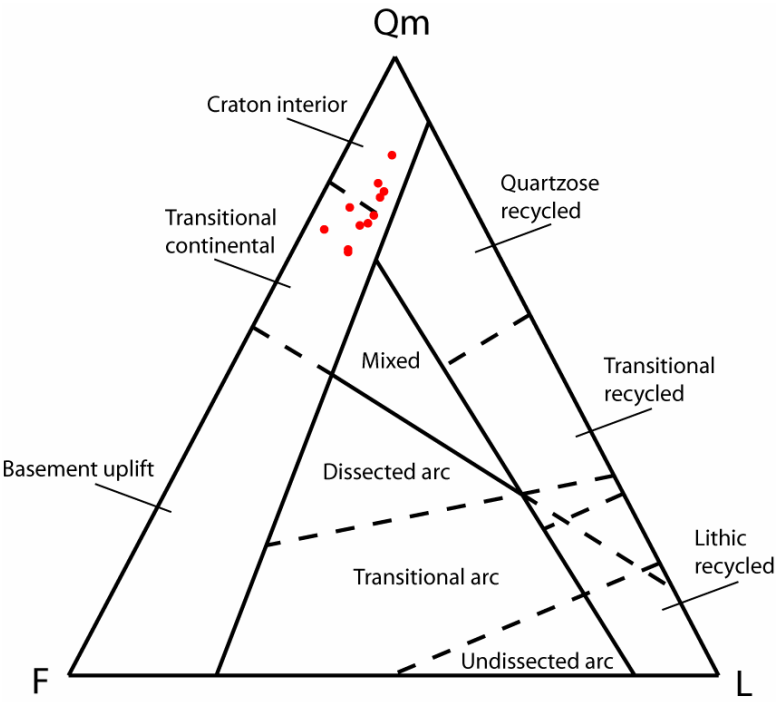

Appendix C. Ternary diagram showing provenance terrains based on sand compositions. This Qm-F-Lt plot includes polycrystalline quartz with lithic grains. Modified from Dickinson (1985).

Facies	Primary Sed. Structures	Secondary Sed. Structures
BCB		convolute bedding
BRL	asymetrical ripple lamination, very small scale trough-cross sets	
SDS	small-scale medium to high angle trough-cross sets	
LDS	large-scale medium to high angle trough-cross sets	
URL	asymetrical ripple lamination, climbing ripples	soft sediment deformation, bioturbation
RLC	symetrical ripple lamination	soft sediment deformation

Appendix D. Table displaying primary and secondary sedimentary structures and the facies they are found in.